2026.01.16
zoom

暗黒物質直接探索のための放射線物性セミナー2025

月出 章

第5回

5. 低速重粒子によるエネルギー付与
5.1. エネルギー分配　核的消光因子
5.2. 電子的LETとBragg-like曲線
5.3. Angular Scattering
5.4. アルファ崩壊の際の反跳重粒子

文献

LLindhard et. al. Mat. Fys. Medd. Dan. Vid. Selsk. **33**, no.10, 1-42 (1963).
Lindhard et. al. Mat. Fys. Medd. Dan. Vid. Selsk. **33**, no. 14, 1-42 (1963).
HMI tables
Hitachi, Mozumder, Nakamura, Phys. Rev. D 105, 063014 (2022).

質問は声でお願いします

内容　　(仮)

5.低速重粒子によるエネルギー付与

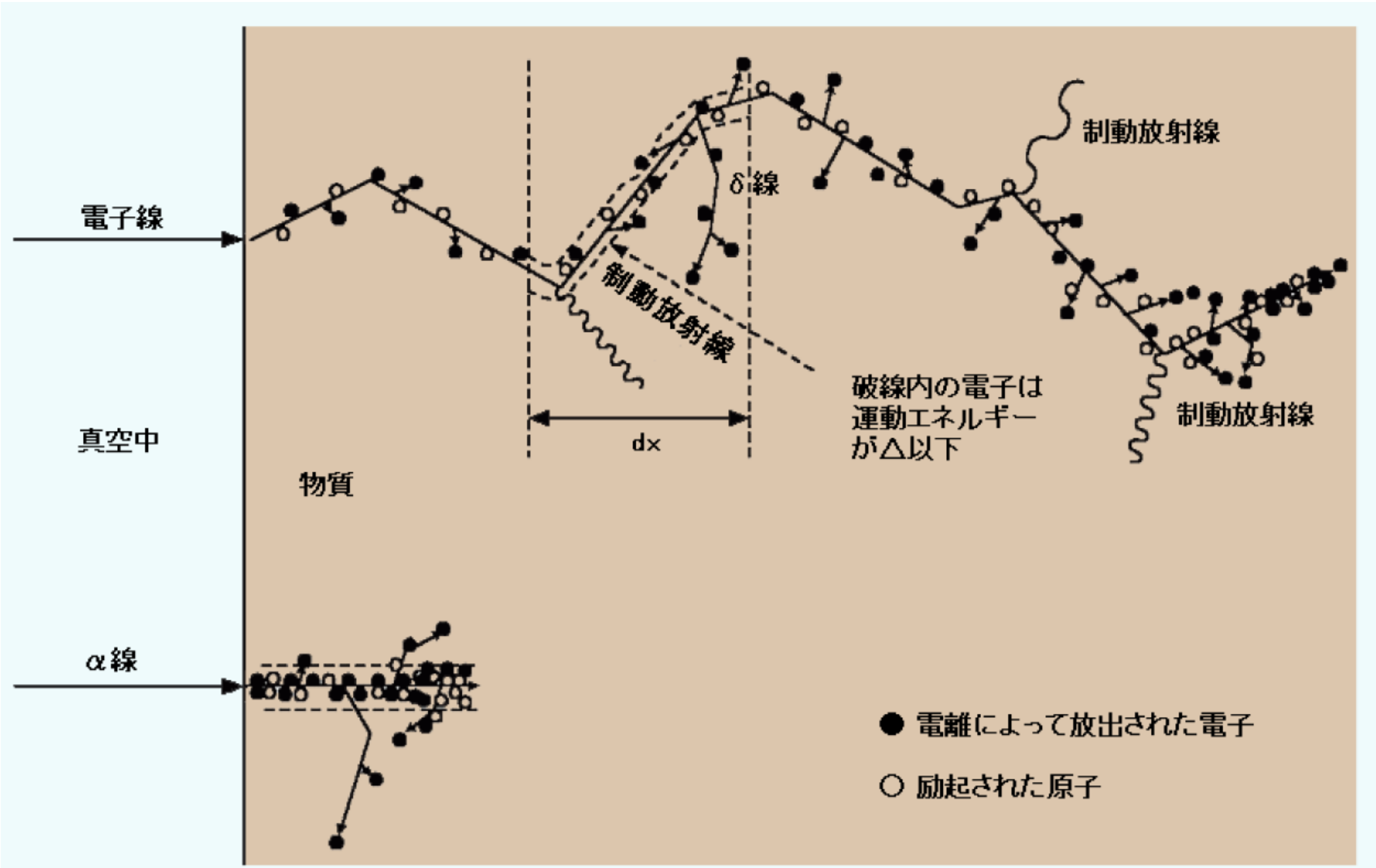

5. 1. エネルギー分配　核的消光因子

Collision cascades

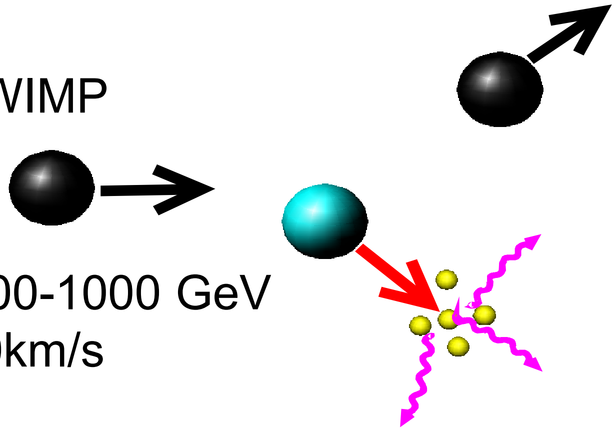

Nuclear quenching factor
(Lindhard factor)

$q_{nc} = \eta/\varepsilon$

電子励起に使われるエネルギーの割合

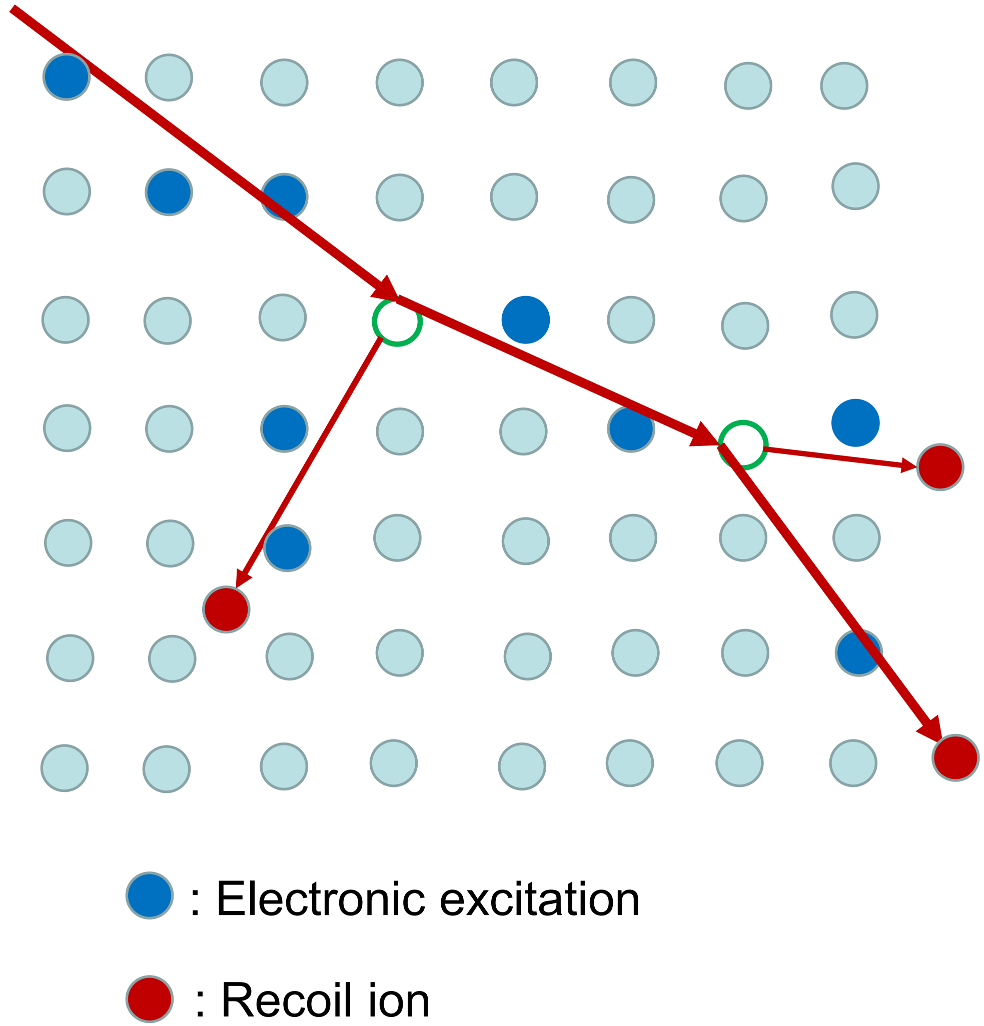

低速重粒子によるエネルギー分配と検出器

電離・発光・熱に費やされるエネルギーの割合が
粒子とエネルギーによって異なる
⇒　主なBGであるガンマ線と反跳核との弁別

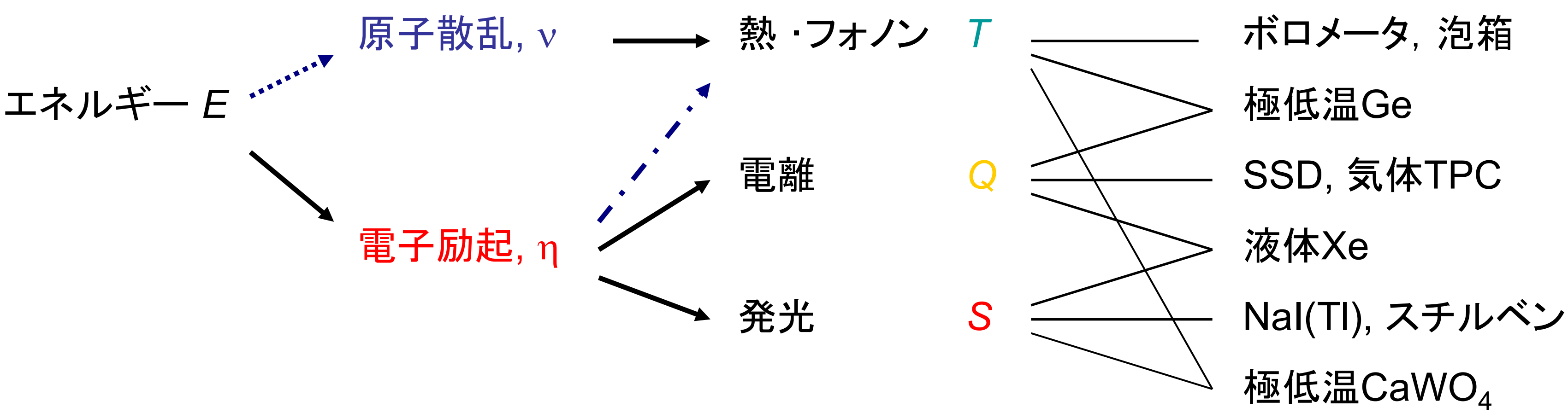

Lindhard factor

核的消光因子 q_{nc} = $\dfrac{\text{電子励起のエネルギー}}{\text{入射粒子のエネルギー}} = \dfrac{\eta}{E}$　　電離・発光を利用する検出器

衝突カスケードが終了した後、電子励起に費やされる エネルギーの割合

RN/γ 比　　気体・半導体

Bragg-like曲線 ($-d\eta/dR_{prj}$)　気体TPC中の電荷分布　head-tail検出

シンチレータのRN/γ 比の考察　$q_T = q_{nc} \cdot q_{el}$

消光なし $q = 1$,　全消光　$q = 0$

Lindhard factor　η/ε

The stopping powers contain only a part of the necessary information to obtain the quenching factor, η/ε ratio. The differential cross section in nuclear collisions is needed for the integral equations.　For $Z_1 = Z_2$,

$$\left(\frac{d\varepsilon}{d\rho}\right)_e \cdot \nu'(\varepsilon) = \boxed{\int_0^{\varepsilon^2} \frac{dt}{2t^{3/2}} \cdot f(t^{1/2})} \cdot \left\{ \nu\left(\varepsilon - \frac{t}{\varepsilon}\right) - \nu(\varepsilon) + \nu\left(\frac{t}{\varepsilon}\right) \right\}$$

$$\left(\frac{d\varepsilon}{d\rho}\right)_e = k\varepsilon^{1/2}$$

$$\left(\frac{d\varepsilon}{d\rho}\right)_n = \int_0^{\varepsilon} dx \frac{f(x)}{\varepsilon}$$

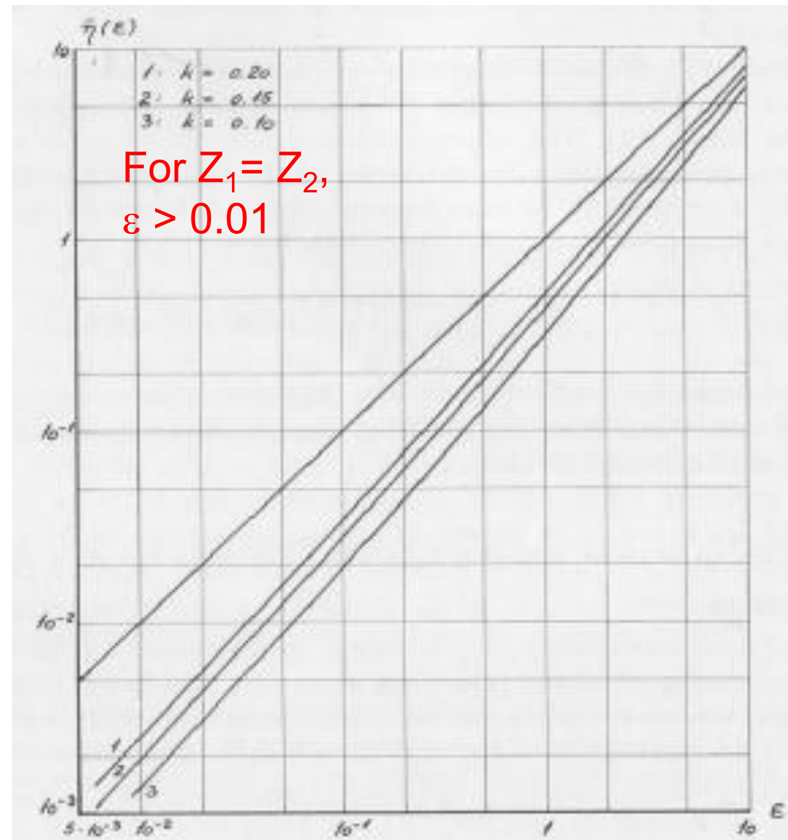

η　as a fn of ε for $k = 0.2, 0.15, 0.1$

上から

低速重粒子(反跳核)の消光因子

全消光因子　(凝縮相)

$$q_{\mathrm{T}} = \int_0^E \boxed{q'_{\mathrm{el}}(E)} \cdot \boxed{q'_{\mathrm{nc}}(E)} \mathrm{d}E \Big/ \int_0^E \mathrm{d}E$$

電子的消光因子

評価には電子励起密度の情報が必要

電子的LET (線エネルギー付与)

$$\mathrm{LET_{el}} = -\frac{\mathrm{d}E_\eta}{\mathrm{d}x}$$

核的消光因子

$$q_{\mathrm{nc}}'(E) \equiv \mathrm{d}\eta/\mathrm{d}\varepsilon = \mathrm{d}E_\eta/\mathrm{d}E$$

① $Z_1 = Z_2$　　Lindhard, 33 (10)

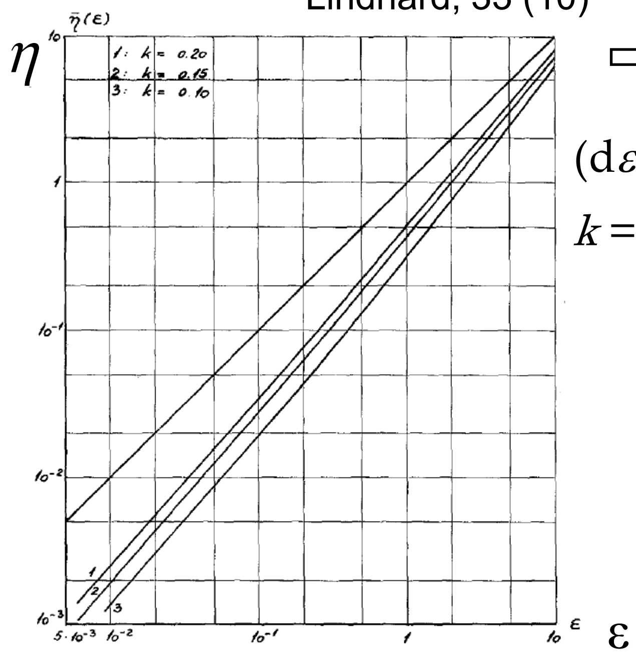

Fig. 3. The function $\bar{\eta}(\varepsilon)$ vs. ε at low values of ε, for $Z_1 = Z_2$ and in the three cases k , 0.15 and 0.20. The curves were computed numerically from (5.1).

$$(\mathrm{d}\varepsilon/\mathrm{d}\rho) \approx k\varepsilon^{1/2}$$

$$k = 0.2,\ 0.15,\ 0.1$$

フィット ⟹

$$\eta = C_1\varepsilon^{P_1} + C_2\varepsilon^{P_2} \qquad q_{nc} = \eta / \varepsilon$$

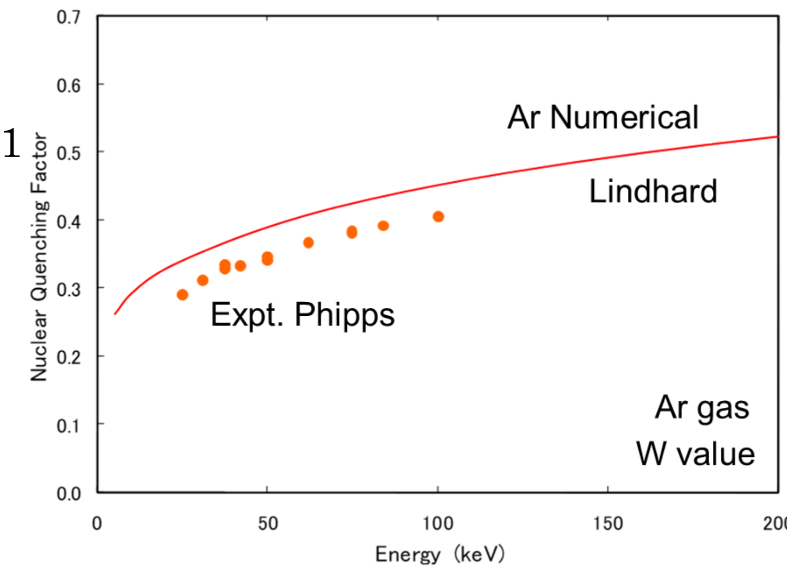

Experimental results for Ar; Phipps et al [1964]

$Z_1 = Z_2$

Table I. Coefficients for the quantity $\eta = C_1\varepsilon^{P1} + C_2\varepsilon^{P2}$ for k values of 0.1–0.2 in the range ~0.01< ε < 10, obtained by fitting the numerical results from Lindhard.

k	C_1	P_1	C_2	P_2
0.10	0.1753	1.0712	0.1358	1.4902
0.15	0.2958	1.1130	0.1304	1.4212
0.20	0.2297	1.0466	0.2768	1.3048

k	ion/atom	C_1	P_1	C_2	P_2	E_L keV	E_H keV
0.127	C/C	0.2428	1.1013	0.1325	1.4521	0.06	55
0.139	Ne/Ne	0.2657	1.1061	0.1371	1.4273	0.2	185
0.145	Ar/Ar	0.2778	1.1085	0.1380	1.4165	0.7	---
0.158	Kr/Kr	0.2303	1.3234	0.2134	1.0738	4	---
0.165	Xe/Xe	0.2361	1.3182	0.2206	1.0730	10	---

5.2. electronic Linear Energy Transfer (LET_{el})

Scintillation as well as its quenching are electronic processes. We introduce the electronic LET.

$LET_{el} \equiv -d\eta/dR = -\Delta\eta/\Delta R$ R: the range

$= -(\eta_1-\eta_0)/(R_1-R_0)$

for quenching calc. etc.

The true range R is given by the total stopping power

$$R_T = \int (dE/dx)_{\text{total}}^{-1}\, dE$$

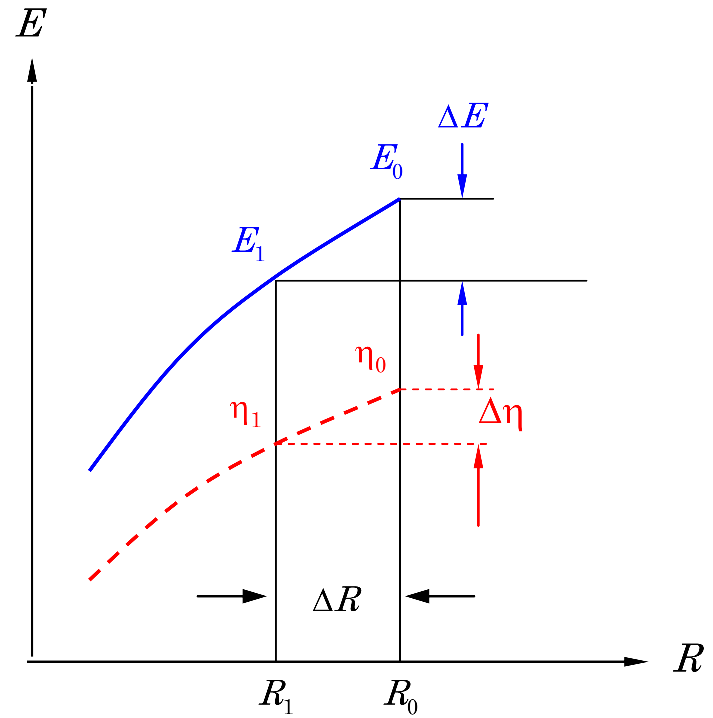

$$\langle LET_{el} \rangle = \eta/R$$

$$\boxed{\mathrm{LET_{el}} \equiv -\frac{\mathrm{d}E_\eta}{\mathrm{d}x} = -\frac{\mathrm{d}E_\eta}{\mathrm{d}E}\cdot\frac{\mathrm{d}E}{\mathrm{d}x} = \frac{\mathrm{d}\eta}{\mathrm{d}\varepsilon}\cdot S_\mathrm{T}}$$

$$\mathrm{LET} = -\frac{\mathrm{d}E}{\mathrm{d}x}$$

The Bragg-like curve for TPC

The projected range, R_{PRJ}, may be used

b) (depth)

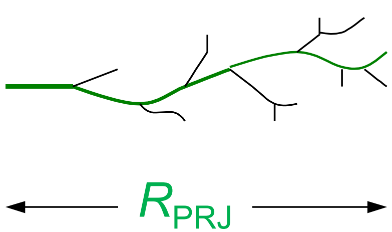

阻止能と電子的LET

$$<\mathrm{LET_{el}}> \equiv -E_\eta / R = q_{nc} <\mathrm{LET}>$$ ⇐ 重粒子の飛程 *R* を求めるのは少し面倒

$$\boxed{\mathrm{LET_{el}} \equiv -\frac{\mathrm{d}E_\eta}{\mathrm{d}x} = -\frac{\mathrm{d}E_\eta}{\mathrm{d}E}\cdot\frac{\mathrm{d}E}{\mathrm{d}x} = \frac{\mathrm{d}\eta}{\mathrm{d}\varepsilon}\cdot S_\mathrm{T}}$$

$$\eta = C_1\varepsilon^{P_1} + C_2\varepsilon^{P_2}$$ ⇐ 解析的に表わせられる。
R は要らない

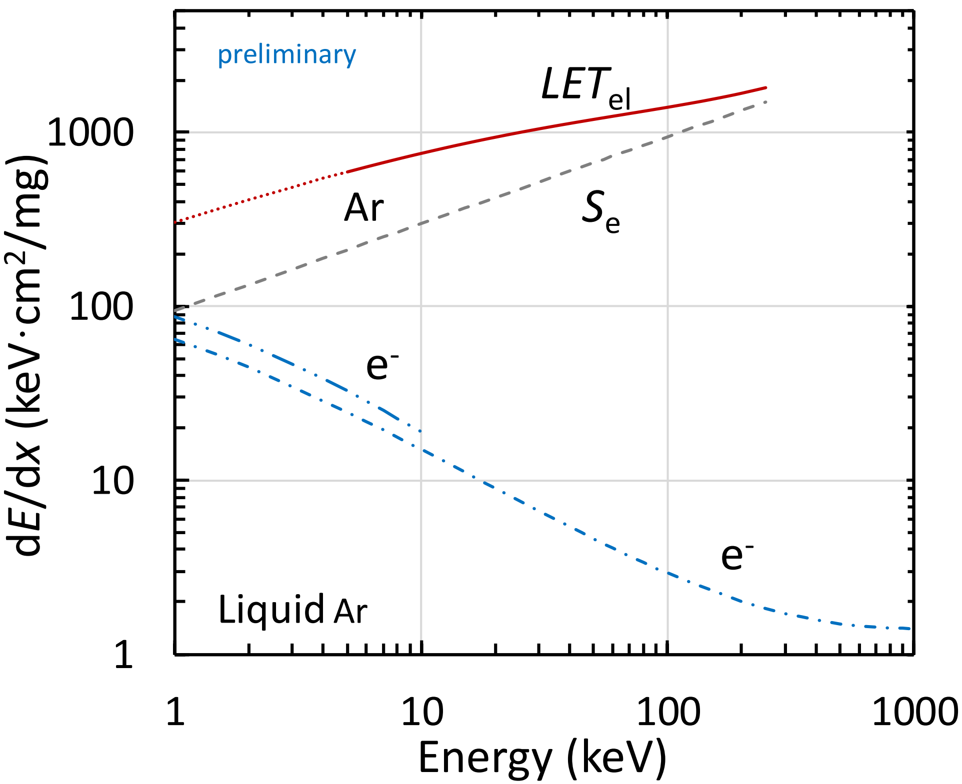

FIG. The electronic stopping power S_e and $\mathrm{LET_{el}}$ for electrons and Ar ions in Ar

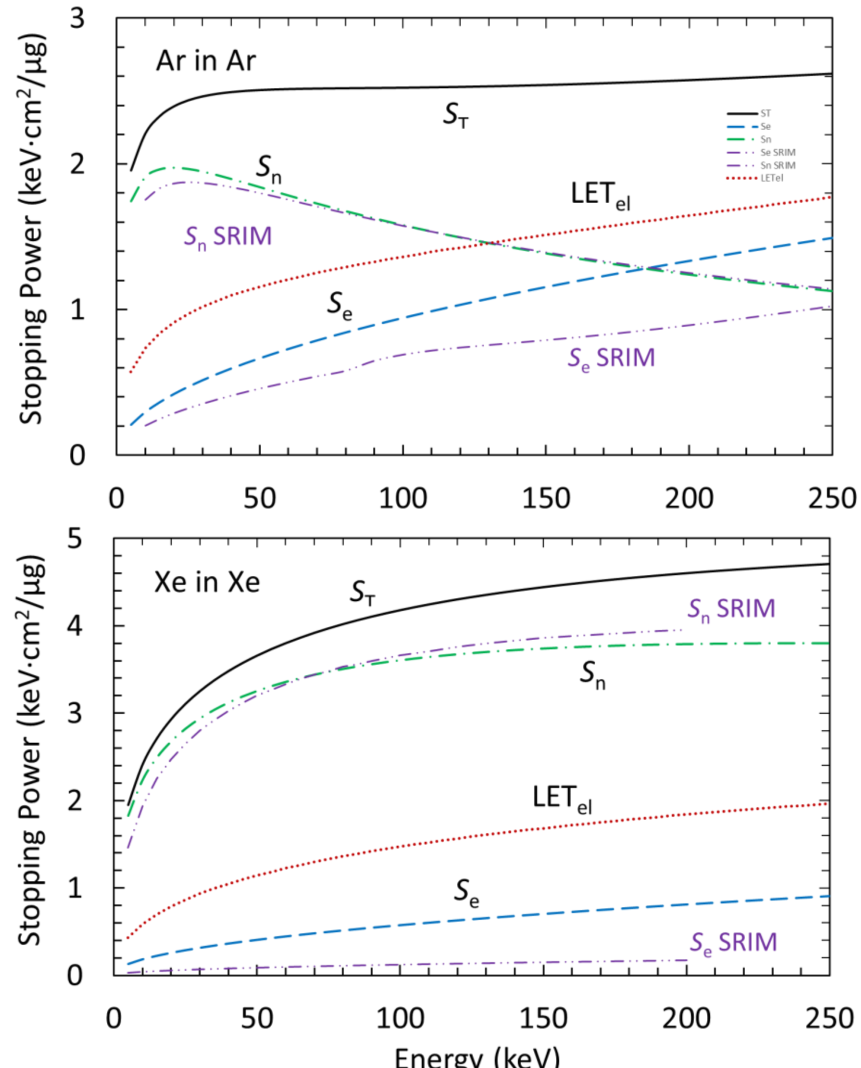

q_{nc}
TRIM との比較

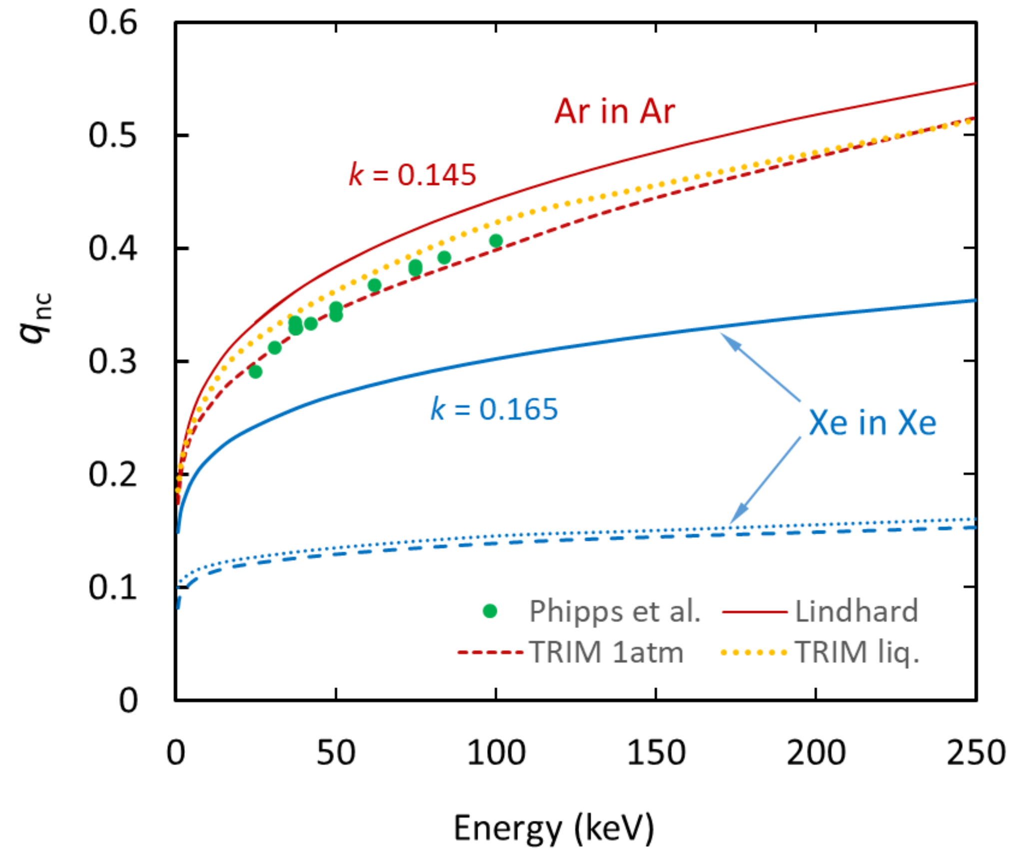

LET_{el} を使うと

LET_{el} を使うと
放射線物理・放射線化学の
情報を使って消光因子を評価できる。

高速重粒子のS_e 依存性
⇓
低速重粒子の LET_{el} 依存性

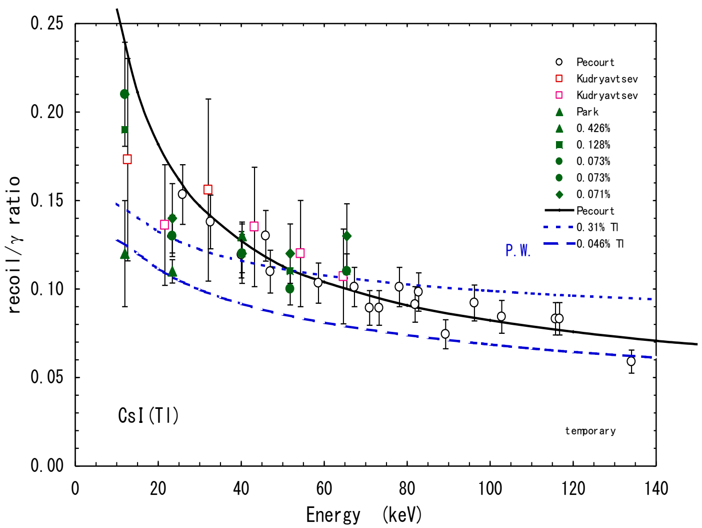

Fig. 4 The recoil ion to γ ratio in CsI(T) as a function of recoil ion energy. The broken lines are present estimates. The solid line is fitting to the Birks–Lindhard model by Pecourt.

The same q_{nc} as LXe.

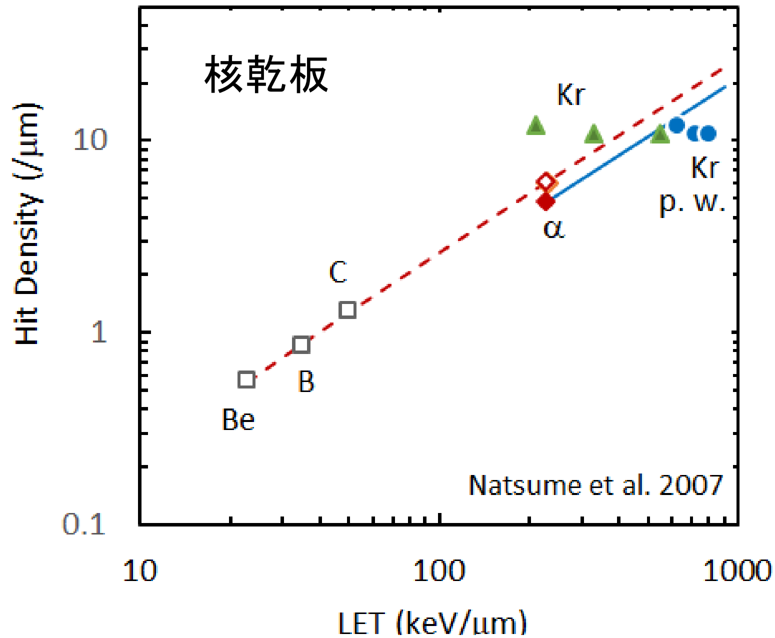

FIG. 5. The mean hit density measured for 5.3 MeV α particles, 290 MeV/n Be, B, and C ions, and 200, 400, and 600 keV Kr ions in fine-grain nuclear emulsion as a function of LET (Fig. 4 in Ref. [17]). The electronic stopping power at incident energy was used for Kr ions (green triangle) [17]. Circles for Kr are replotted at averaged LET_{el} (blue circle; present work, see the text). Open and closed symbols show the difference in the process with the standard developer and the fine-grain developer, respectively.

Lindhard factor in compounds

No expressions for q_{nc} in compounds are available. We use a simple approximation.

An independent element approach

$$q_{nc}(C/CS_2) \approx q_{nc}(C/C)$$

$$q_{nc}(S/CS_2) \approx q_{nc}(S/S)$$

The model should be tested in ionization measurements in gas.

The simple approach is possible since S_e/S_T ratios for collisions with homo- and hetero-atoms are close to each other

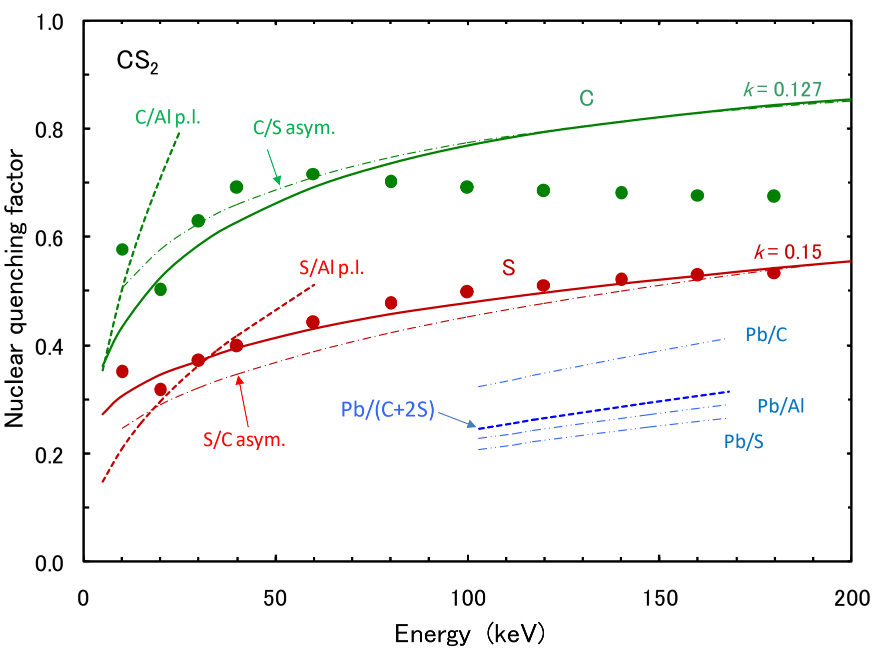

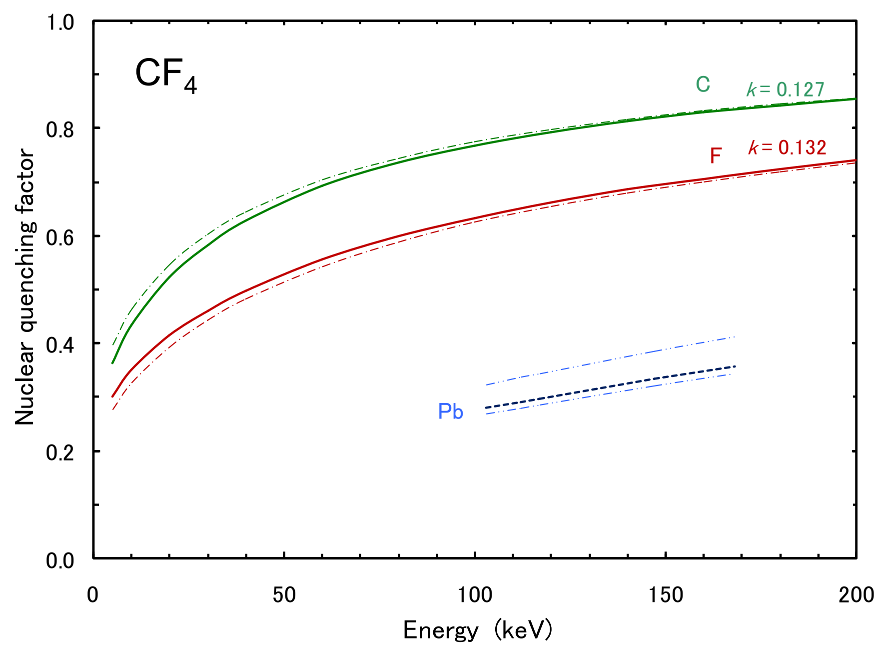

●,●; expt. & part simulation by Snowden-Ifft

NIMA 498, 155 (2003)

Solid curves; the independent element approach

Inorganic Scintillators

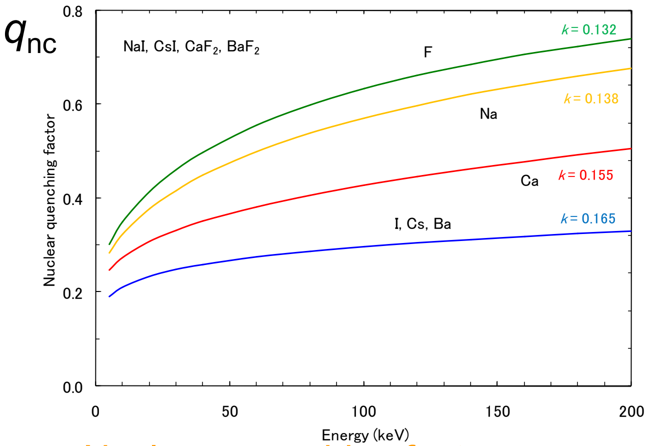

Fig. Nuclear quenching factor q_{nc} for recoil ions in NaI, CsI, CaF_2 and BaF_2 as a function of recoil ion energy.

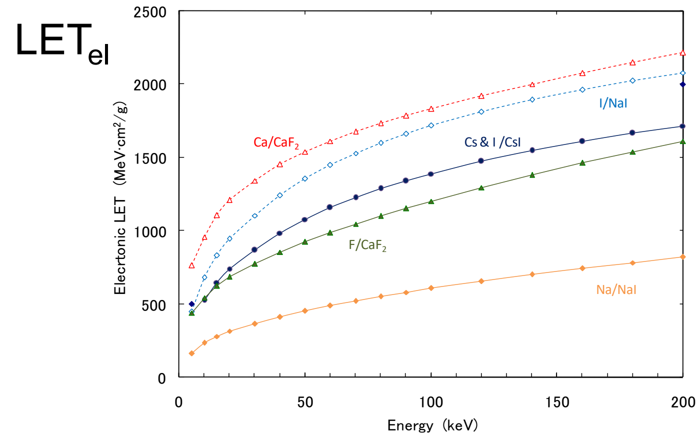

Fig. Electronic LET for recoil ions in NaI, CsI and CaF_2 as a function of energy.

上段
低速重粒子

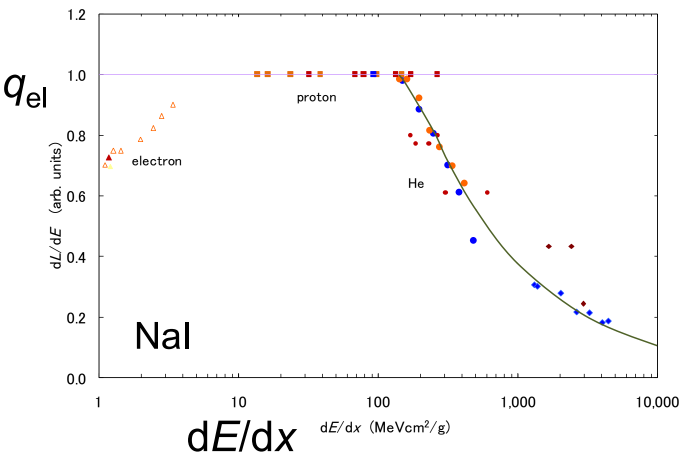

Fig. Scintillation efficiency for various particles as a function of LET in NaI(Tl). The horizontal bars show regions of electronic LET for recoil ions. Murray & Meyer, PR 122, 815 (1961).

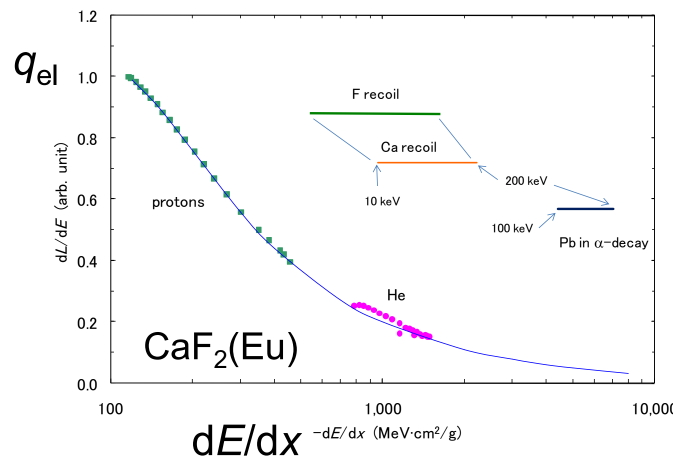

下段
高速重粒子

Fig. Scintillation efficiency for protons and He ions (Zhang,2008) as a function of differential LET in CaF_2(Eu). Horizontal bars show electronic LET (=-dh/dx) for recoil ions.

Quenching factor for Inorganic Scintillatiors

$$RN/g = q_T/L_g = (q_{nc} \cdot q_{el})/L_g$$

$$q_{nc} \Rightarrow LET_{el} \Rightarrow q_{el}$$

Scintillation efficiency L_g in NaI depends on LET and the velocity. We take values for slow ions

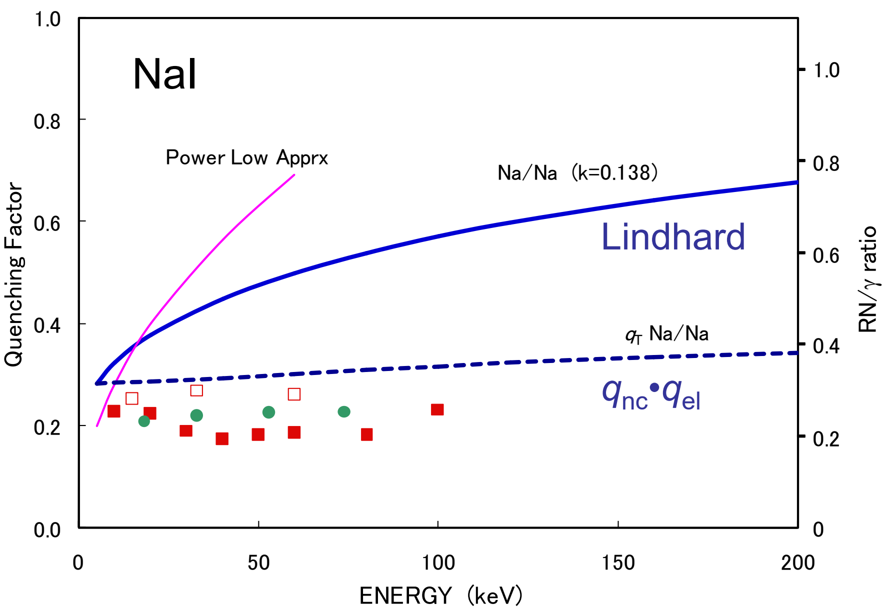

Fig. q_{nc} for recoil Na ions in NaI(Tl).
■□:Sheffield, ●:Gerbier

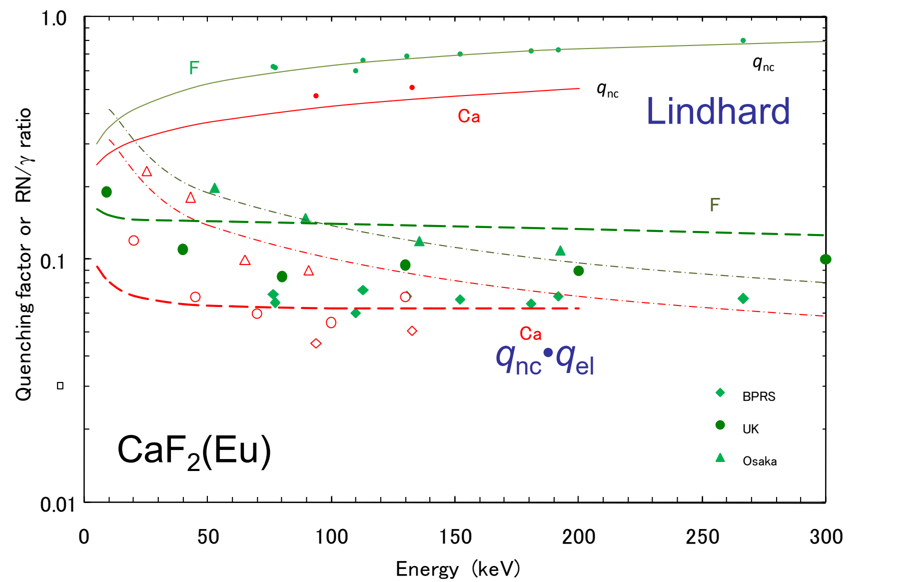

Fig. The nuclear quenching factor, q_{nc}, and RN/g ratios for Ca and F ions in CaF_2(Eu) as a function of recoil ion energy.
Solid curves are q_{nc} (p.w.).
Broken curves are RN/g ratio (p.w.).
Small dots represents q_{nc} using TRIM code (BPRS).
The dot-dashed curves are RN/γ ratio, fitting and extrapolated to the low energy region assuming that the q-value depends inversely on S_T (Osaka).

Can depends on sensitizer [Tl] concentration.

5.2. 方向感応型検出器

一般の検出器は季節変動
しか検出できない
季節変動は極めて小さい。

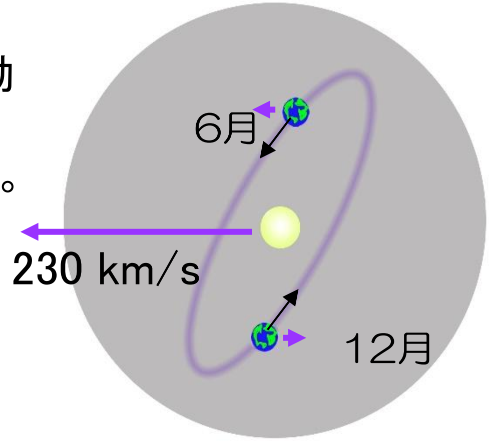

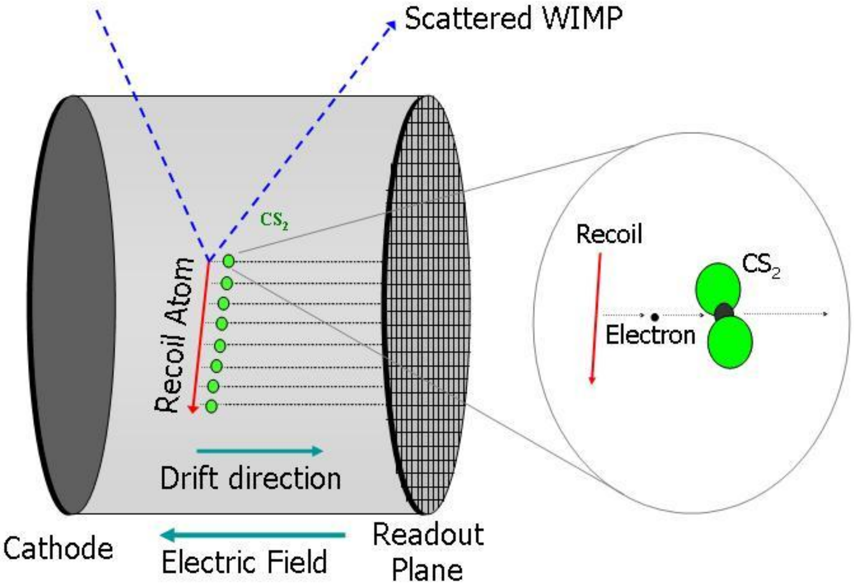

DRIFT

気体TPC (Time Projection Chamber)
CS_2 のような電気陰性のガスを使う。(拡散が小さい)

飛跡検出器　fine grain emulsions

はくちょう座

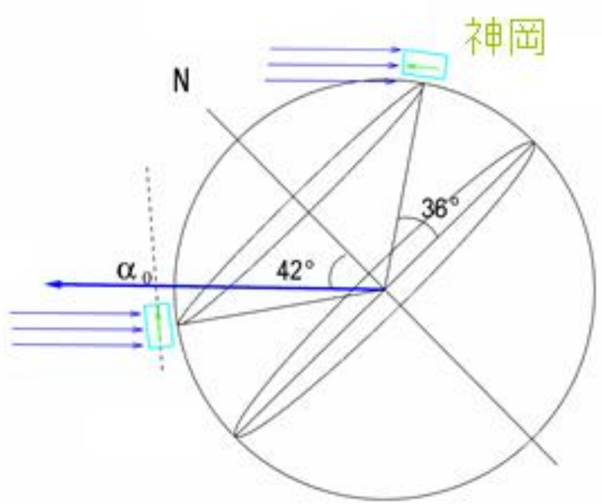

方向感度をもった検出器は
日変動が観測できる。

反跳核の飛程は極めて短い
散乱により前後の判定が難しい

5. 2. 電子的LETとBragg-like曲線

The ranges, R & R_{prj}

飛程

$$R \cong \int_0^E \frac{\mathrm{d}E'}{N_a \cdot S_T}$$

R_{prj} : projected range

$$R / R_{\mathrm{prj}} \cong 1 + \psi \frac{M_2}{M_1}$$

$R_\perp$: range projected on the plane
$\perp$ to the initial direction

R_c : chord range

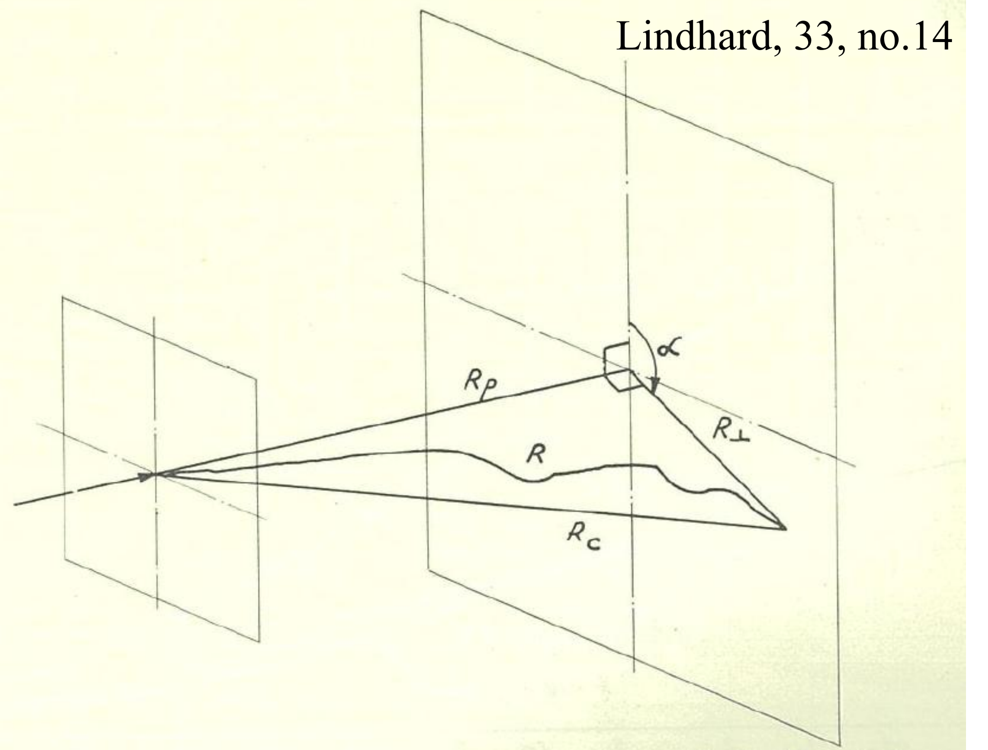

Fig. 10. Sketch illustrating definition of range concepts R, R_p, R_c and $R_\perp$.

方向感度をもつ検出器

電子的 Energy の空間分布
励起状態分布

$\mathrm{LET_{el}} = -\mathrm{d}E\eta/\mathrm{d}x$
飛跡に沿った電子的 Energy

$\mathrm{LET_{el}^{prj}} = -\mathrm{d}E_\eta/\mathrm{d}R_{\mathrm{prj}}$

$\mathrm{LET_{el}^{c}} = -\mathrm{d}E_\eta/\mathrm{d}R_\mathrm{c}$ ← 個々の反跳核
測定に関係するのはこちら

電荷量 ⇒ Energy
始点と終点の距離 ⇒ R_C

The ranges, R & R_{prj} GasTPC

MS. VI, C. p.10-11

The rule of thumb

$$R/R_{prj} \cong 1 + \frac{1}{3}\frac{M_2}{M_1} \quad \Rightarrow$$

Lindhard, 33, no.14

$$\boxed{R/R_{prj} \cong 1 + \psi \frac{M_2}{M_1}}$$

k : electronic stopping constant

$$(d\varepsilon/d\rho) \approx k\varepsilon^{1/2}$$

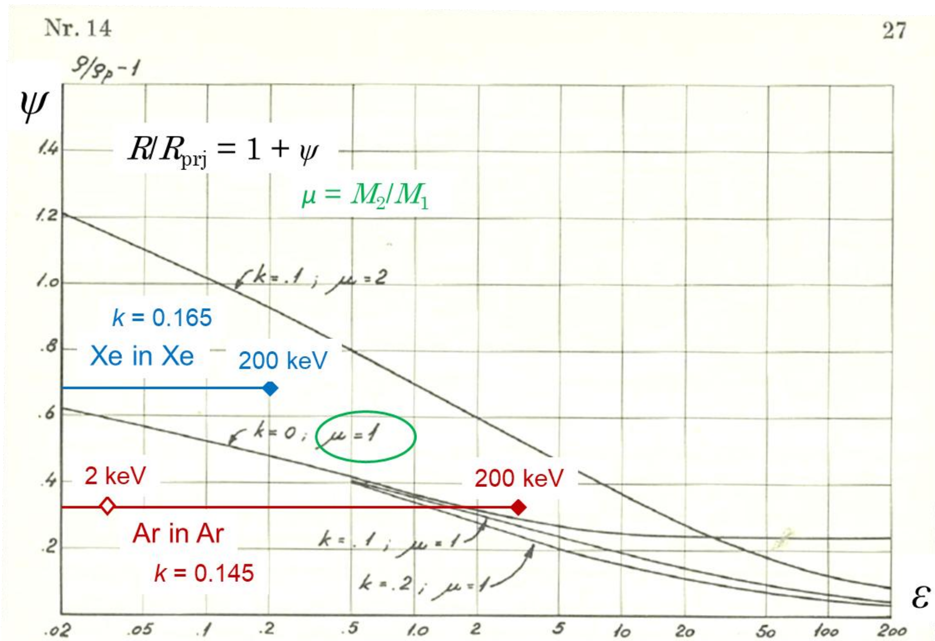

Fig. 9. Approximate curves for $\bar{\varrho}_1/\bar{\varrho}_{p1}$ for large values of the ratio $\mu = M_2/M_1$ and a few values of k.

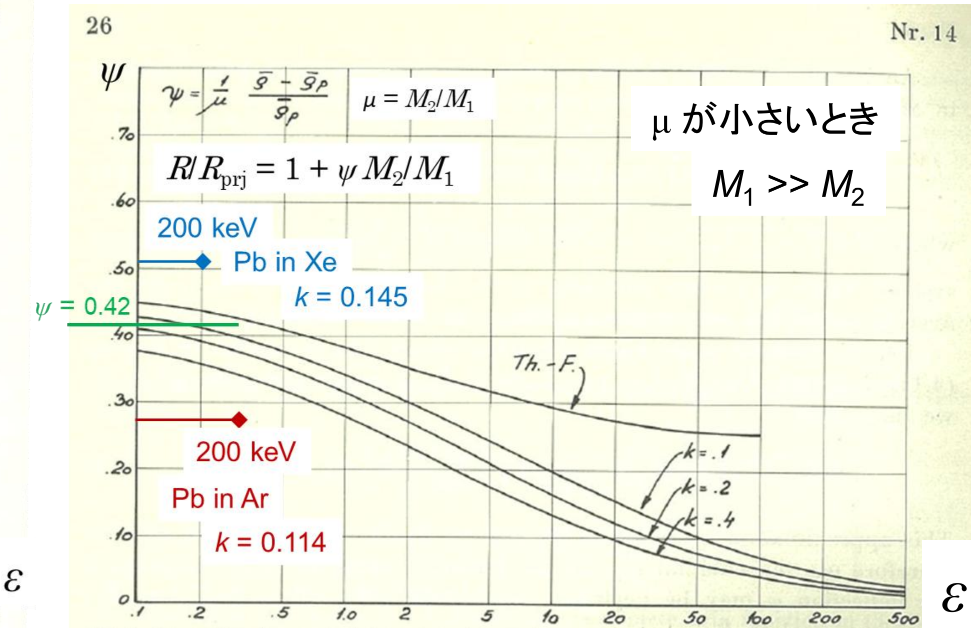

Fig. 8. Correction for projected ranges $(\bar{\varrho}_1 - \bar{\varrho}_{p1})/\bar{\varrho}_{p1} = \mu\psi$, to first order in the mass ratio $\mu = M_2/M_1$. Curves are shown for pure nuclear stopping and for three values of electronic stopping parameter k.

$k = 0.15$

$$\psi = 0.0089x^3 - 0.0437x^2 - 0.1127x + 0.6193$$

$$x = \log(\varepsilon/2) + 2$$

$\Psi \approx 0.42$

The ranges, R & R_{prj}

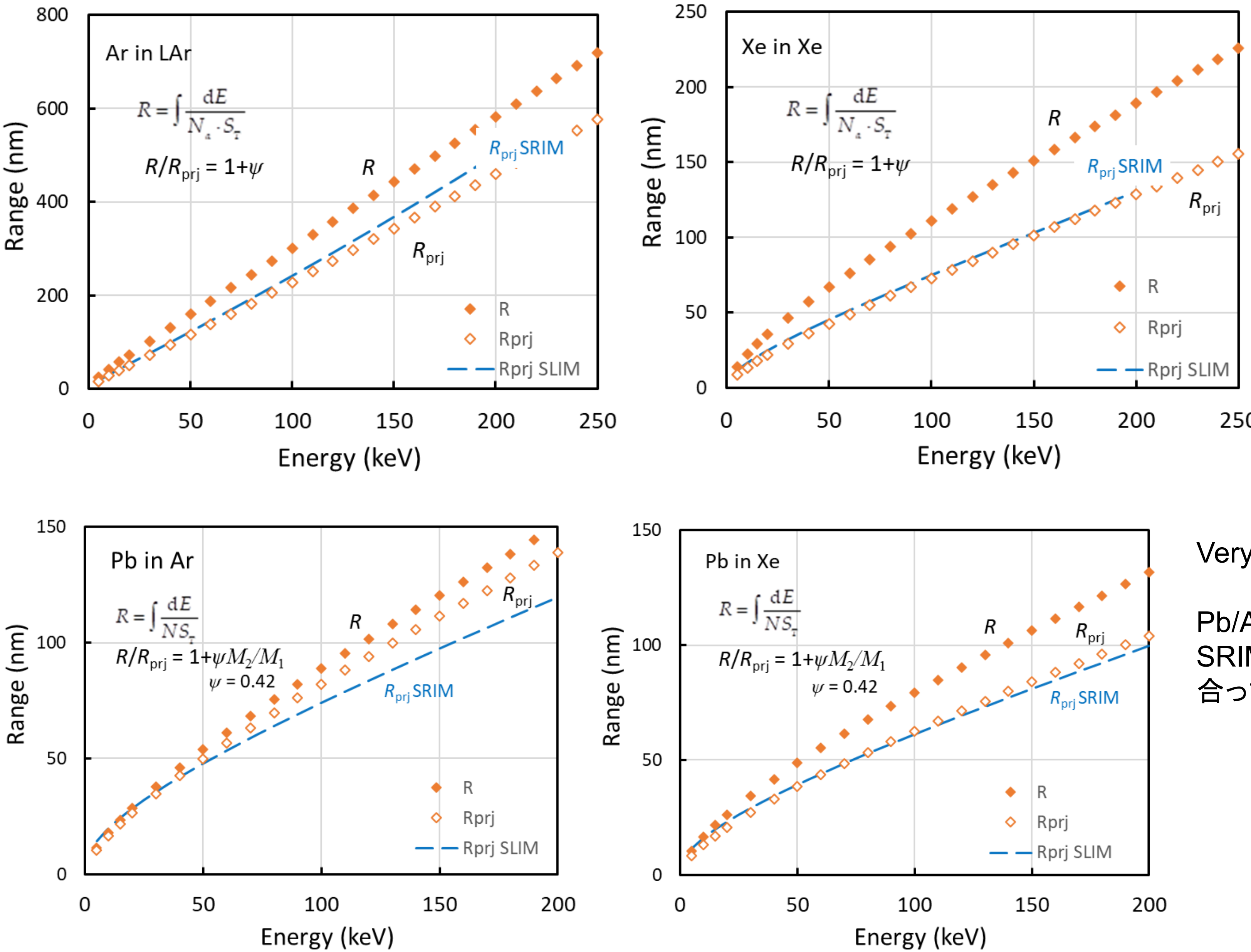

Very Low Energy
を除くと
Pb/Ar 以外は
SRIM（青）と概ね
合っている

深さ方向の励起種分布

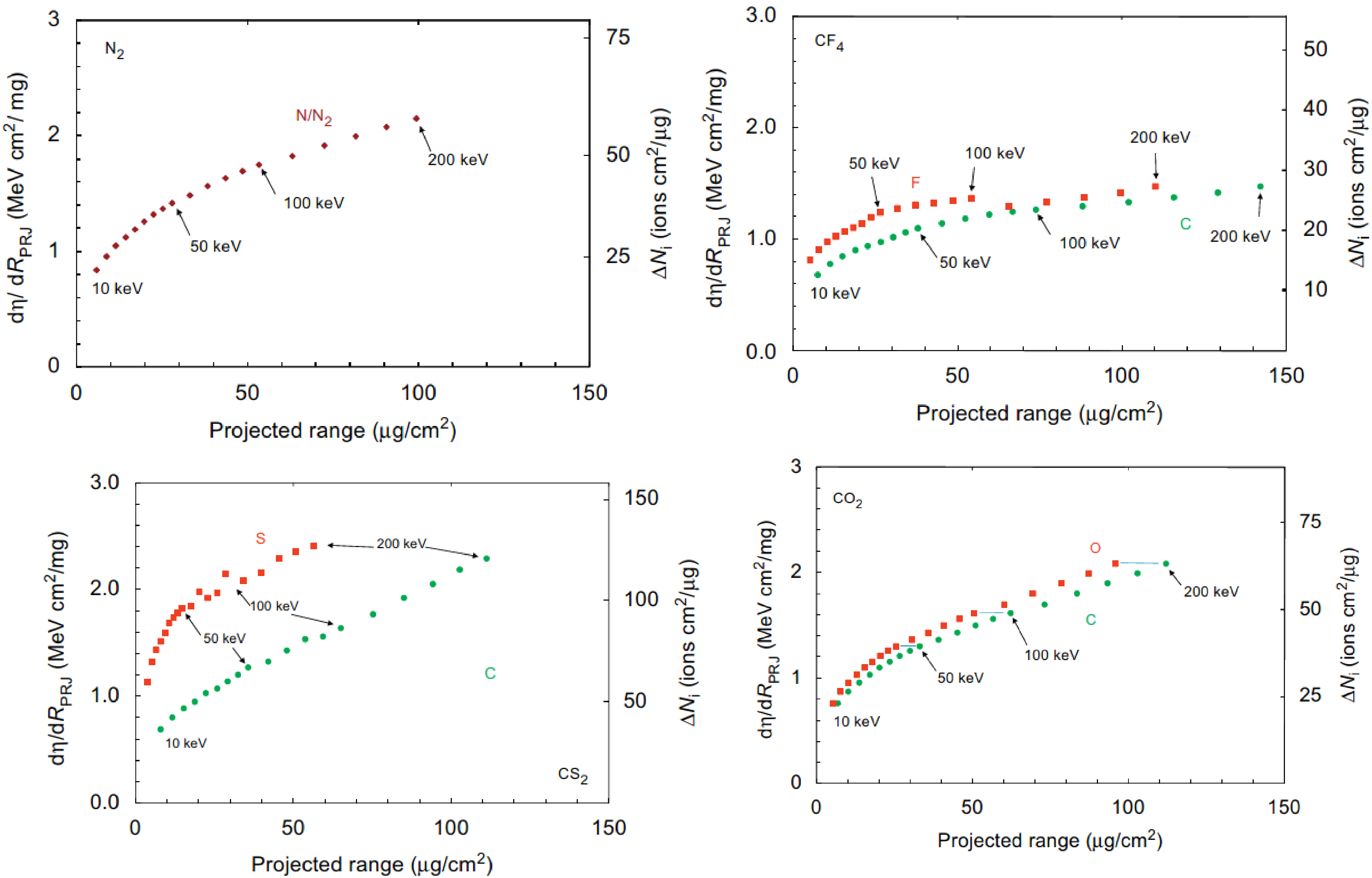

R_{prj} はSRIM

Radiation Physics and Chemistry 77 (2008) 1311–1317

Bragg-like curve $d\eta/dR_{PRJ}$

charge distribution in recoil direction

Head-Tail CS_2 CF_4

CS_2

low diffusion CS^- ions

release e^- at the anode and

get electron multiplication

CF_4

charge carrier is electron

F is effective for WIMP search

via spin-dependent interaction

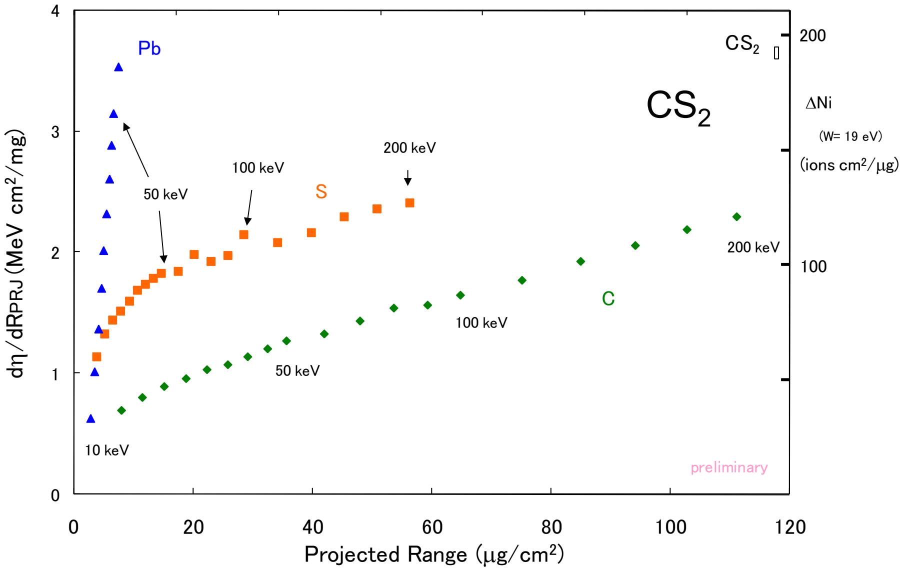

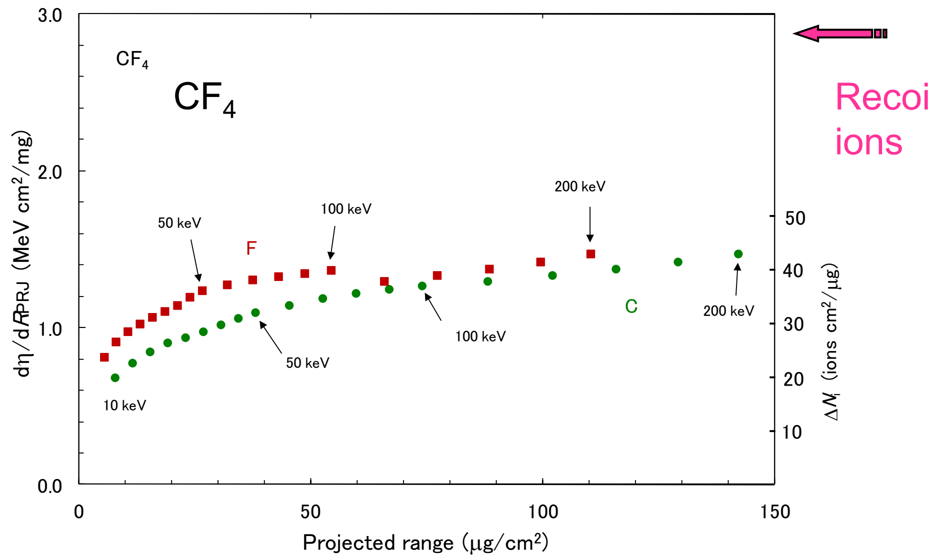

Straggling と Lindhard 因子 q_{nc} の影響

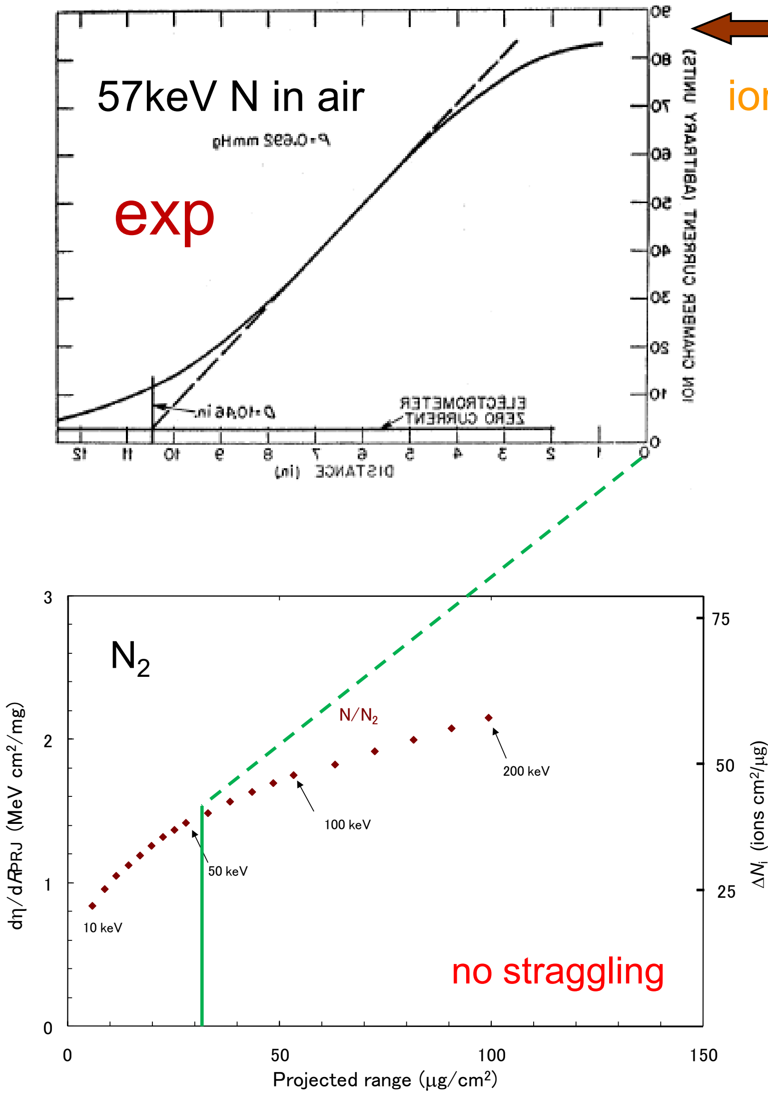

Hitachi, Rad. Phys. Chem. 77, 1311-1317 (2008)

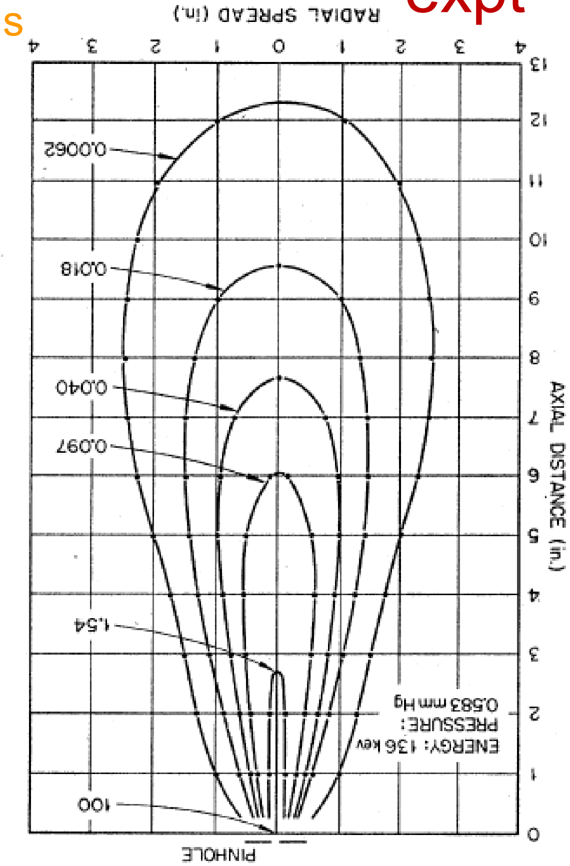

136 keV Ar in Ar

Evans, PR 90, 825 (1953)

q_{nc} を考慮していない

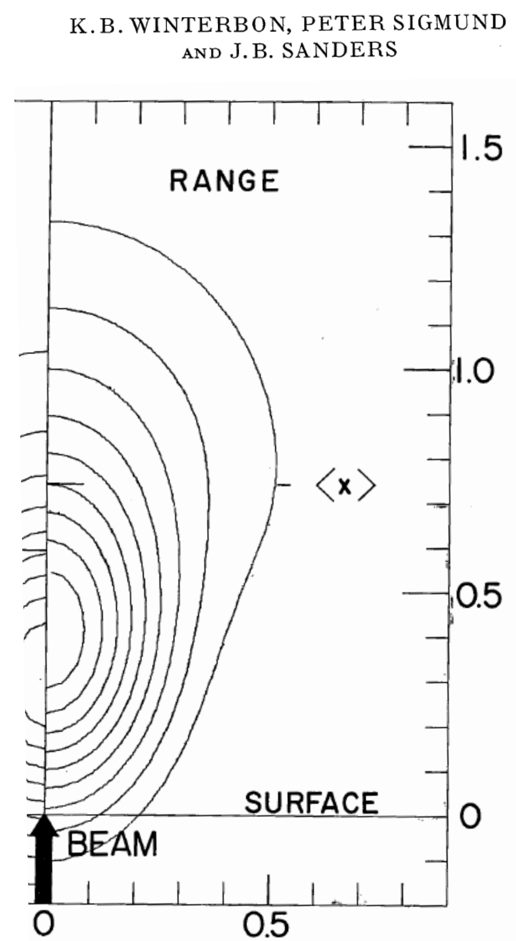

$\Delta R_{\perp}$ ⇒ bell shape

$\Delta R_{\perp}$ & $\Delta R_{//}$ ⇒ drop-shape

Head-Tail CF_4

F: 核スピンの断面積アリ

核的消光因子 q_{nc}

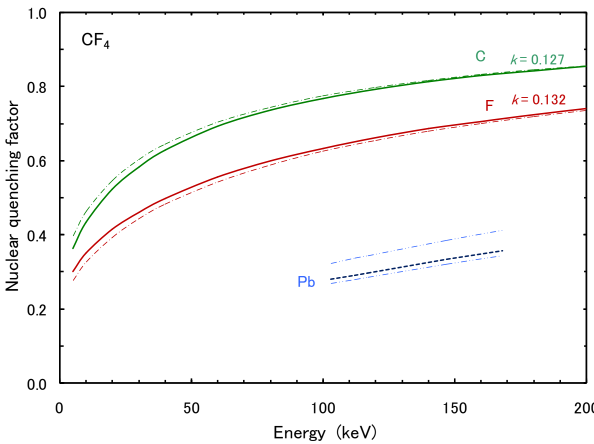

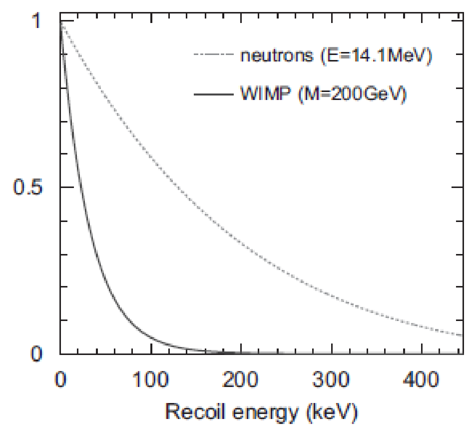

CCDカメラ

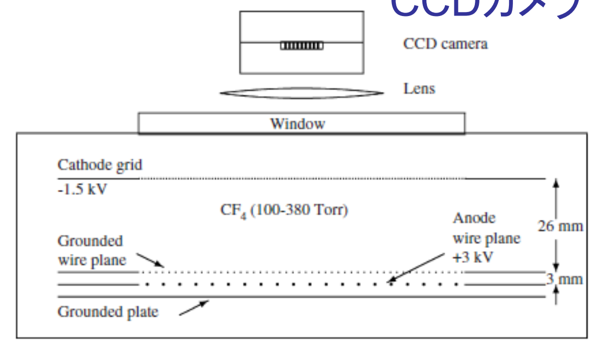

CF_4

中性子

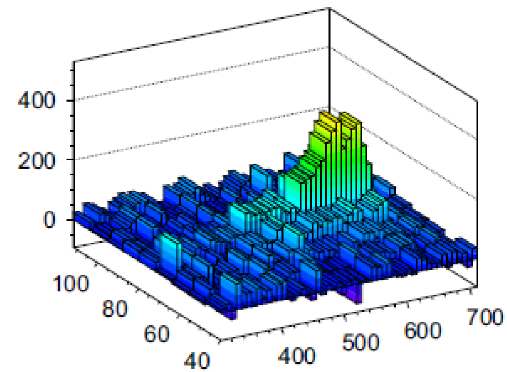

Bragg -like曲線 $d\eta/dR_{PRJ}$

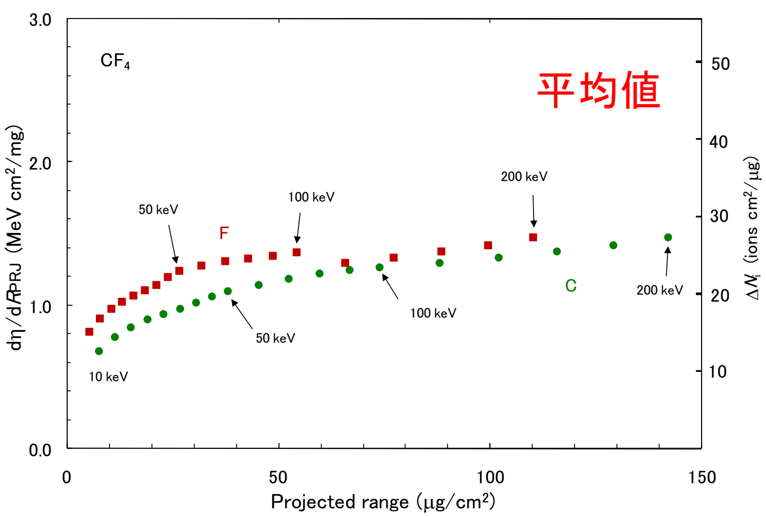

反跳核

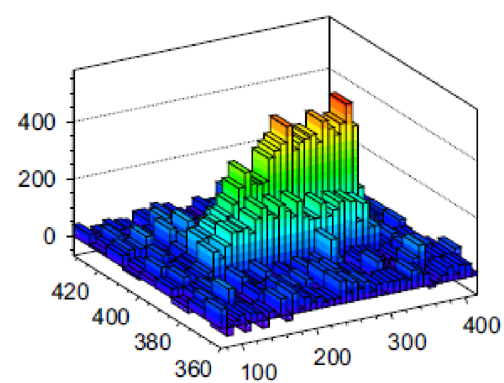

Hitachi, Rad. Phys. Chem: ASR2007

DMTPC, Dujmic, NIMA 584, 327 (2008)

5.3. Angular scattering

反跳核の多重散乱による散乱角の評価方法

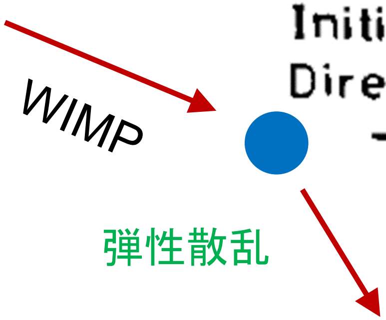

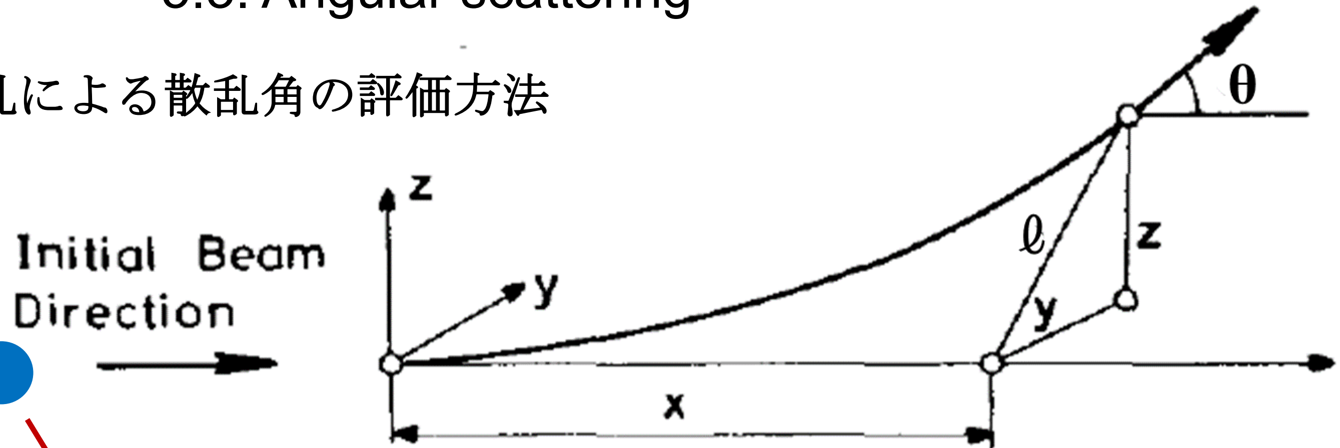

Multiple Scattering

a. 簡易式
Bohr-Williams, SRIM Table？ $E\eta$ 分布が考慮されない。

b. 標準理論
b1 厚さ x が薄い Meyer, Sigmund & Winterbon $E\eta$ 分布が考慮されない。
b2 厚さを考慮 Valdés & Arista $E\eta$ 分布が考慮されない。

c. Monte Carlo simulation
$E\eta$ 分布？散乱角の定義？
素過程の情報 が重要。

d. Range & Projected range, LET_{el}
標準理論に $E\eta$ 分布を考慮。

$E\eta$ 分布 付与された電子的エネルギー

Electronic linear energy transfer
$LET_{el} = - dE_{\eta}/dx$

簡易評価

角度散乱 Ψ の簡易式 （Bohr-Williams）

HMI tables

$$\left\langle \Psi^2 \right\rangle = \left\langle \Omega^2 \right\rangle \cdot N \cdot x = \frac{A_2}{A_1}\frac{S_n}{E}x$$

Ω^2 : 角度散乱断面積
S_n : 核的阻止能
N : 原子密度, x : 厚さ
入射 : Z_1, A_1, 標的 : Z_2, A_2

散乱角と横方向距離

$$\theta = \Gamma_m \frac{\ell}{x}$$

θ : 散乱角
$\ell^2 = y^2 + z^2$
x : 厚さ
$\Gamma_\mathrm{m} = 1.8 \sim 2.3$

角度散乱Ψ ⇔ 横方向ストラグリング$R_\perp$
S_n

$$R / R_\mathrm{prj} \cong 1 + \frac{1}{3}\frac{A_2}{A_1}$$

縦方向ストラグリング $\Delta R_{//}$ S_n & S_e

$$\left(\frac{\Delta R_{//}}{R}\right)^2 \approx \frac{2}{3}\frac{A_1 A_2}{(A_1 + A_2)^2}$$

SRIMはこれを使用（標的による）？

Lindhard et al.

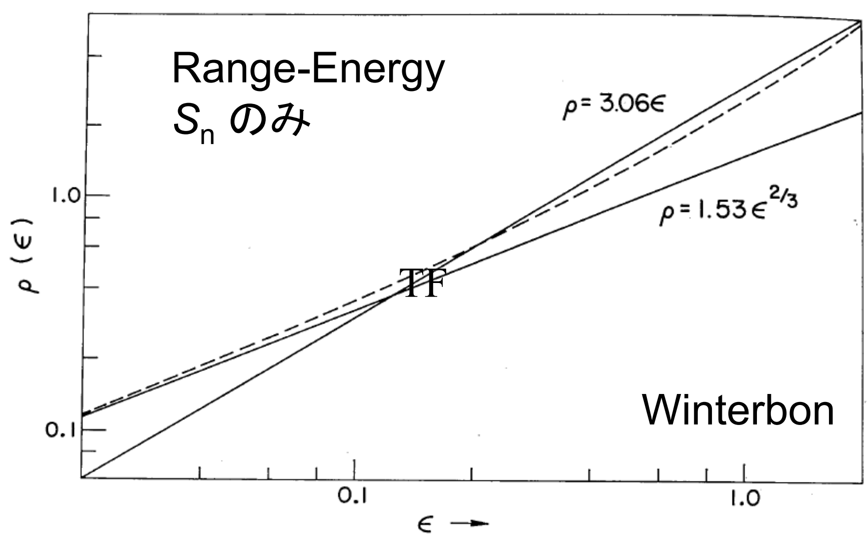

標準理論

$$\mathrm{d}\sigma = \frac{\pi a^2}{2} t^{-3/2} f(t^{1/2})\mathrm{d}t \qquad \tau = \frac{a_s^2}{r_0^2} n_c = \pi a_s^2 N x$$

$$t^{1/2} = \varepsilon \sin(\vartheta / 2)$$

ϑ : Reduced angle
τ : Reduced thickness
$r_0 \approx N^{-1/3}/2$
n_c : no. of collisions

Meyer, Sigmund & Winterbon
Thomas-Fermi interaction
Lenz-Jensen interaction

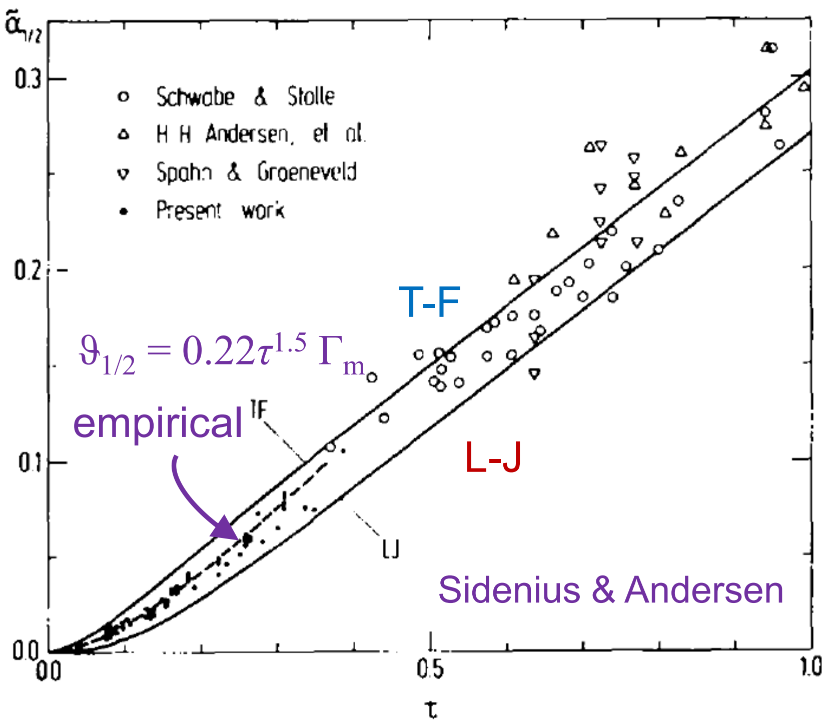

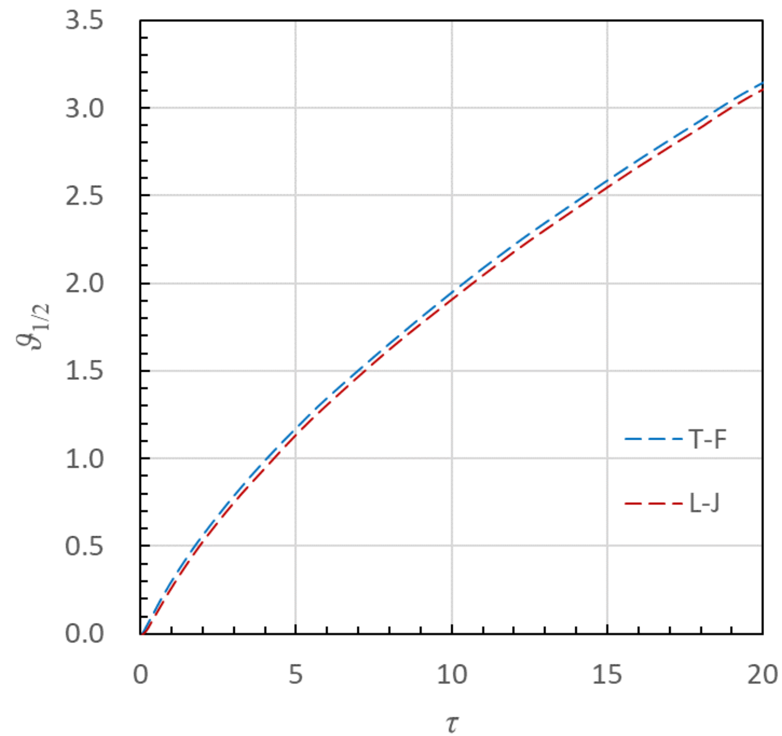

TFとLJの中間をとる。

Theories

Meyer based on Thomas-Fermi interaction

$$\vartheta_{1/2} = g_1(\tau) + \frac{a^2}{r_0^2} g_2(\tau) \qquad \tau = \frac{a_s^2}{r_0^2} n = \pi a_s^2 N x$$

ϑ : Reduced angle
τ : Reduced thickness

$$\vartheta_{1/2} \approx g_1 = -1.936\times10^{-5}\tau^4 + 1.005\times10^{-3}\tau^3 - 2.004\times10^{-2}\tau^2 + 0.3177\tau$$

Sigmund & Winterbon
Thomas-Fermi interaction
Lenz-Jensen interaction

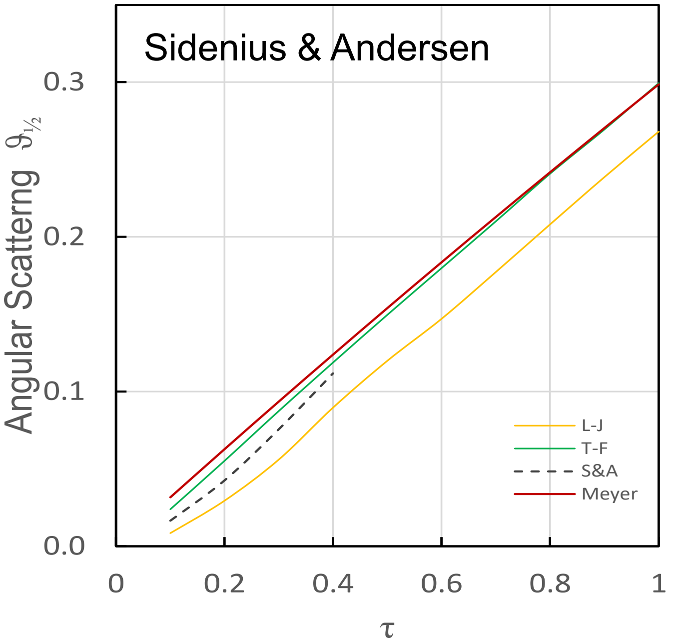

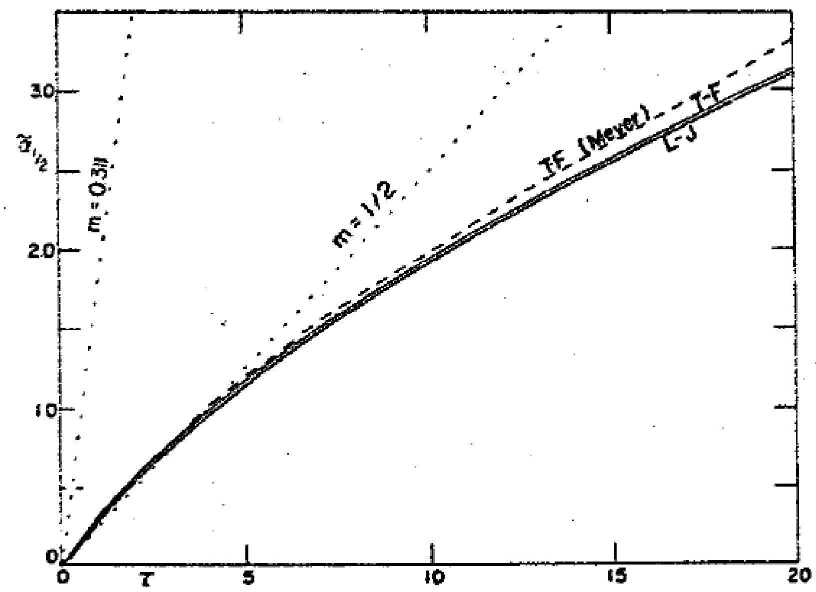

Angular scattering and lateral straggling

The lateral displacement and the scattered angle θ are interrelated

$$\theta = \Gamma_m \frac{\ell}{x}$$

Sidenius and Andersen gave an empirical formula

$$\tilde{u}_{1/2} = 0.22\tau^{2.5}$$

$$\tilde{\vartheta}_{1/2} = \frac{\tilde{u}_{1/2}}{\tau}\Gamma_m = 0.22\tau^{1.5}\Gamma_m$$

the reduced and absolute terms

$\ell = (y+z)^{1/2}$: the lateral straggling

$$\theta_{1/2} = \vartheta_{1/2}\frac{2}{\varepsilon}\frac{A_2}{A_1 + A_2}$$

$$u = \pi a_s^2 N \frac{E a_L}{2Z_1 Z_2}\ell$$

θ : the scattering angle

$\ell = (y+z)^{1/2}$: the lateral straggling

x : the thickness

SRIM gives the lateral straggling

$$\tilde{\theta}(R) = \Gamma_m(\tau)\frac{\tilde{\ell}(R)}{R}$$

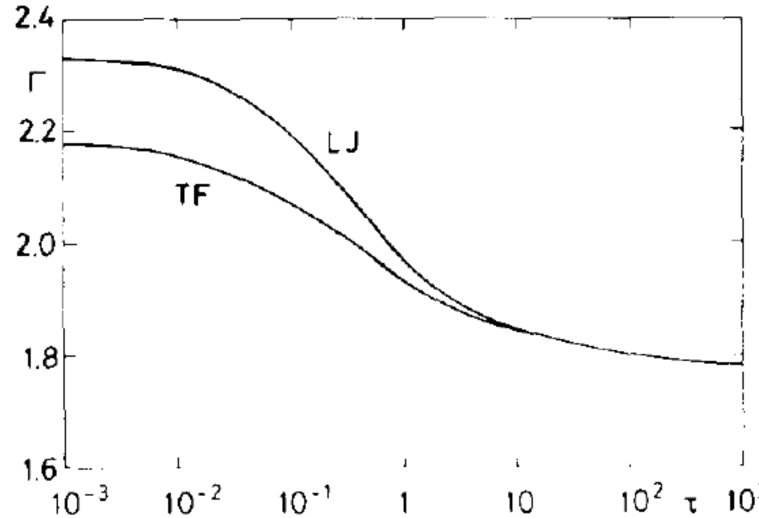

エネルギー損失の効果
厚さを考慮　Valdés & Arista

平均のエネルギー ε_{m} を使って近似

$$\varepsilon_m = \frac{1}{4}\varepsilon_0 (1+\mu^{1/2})^2$$

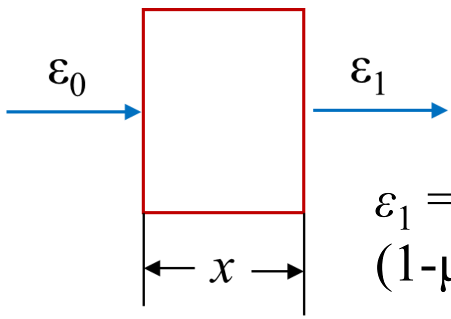

$\varepsilon_1 = \mu\varepsilon_0$

$(1\text{-}\mu) = 0 \sim 0.7$

実験値と経験式 Sidenius & Andersen

$$\vartheta_{1/2} = \frac{u_{1/2}}{\tau}\Gamma_m = 0.22\tau^{1.5}\Gamma_m$$

$$\tau \leq 0.4$$

散乱角 と $E\eta$分布

Range & Projected range, $\mathrm{LET_{el}}$

$Z_1 = Z_2$

q_{nc} を含まず、飛跡の広がりで、電子励起状態の分布ではない。

R_{prj} : projected range

$$R / R_{\mathrm{prj}} \cong 1 + \psi \frac{M_2}{M_1}$$

$$\mathrm{LET_{el}}^{\mathrm{prj}} = -\mathrm{d}E_\eta / \mathrm{d}R_{\mathrm{prj}}$$

$$\mathrm{LET_{el}}^{\mathrm{c}} = \mathrm{LET_{el}}^{\mathrm{prj}} \cdot R_{\mathrm{prj}} / R_{\mathrm{c}}$$

標準理論に $E\eta$ 分布を考慮できる。

$\Delta R_{//}$ を含まない 釣鐘型の分布

（$\Delta R_{//}$ を含むと水滴型に）

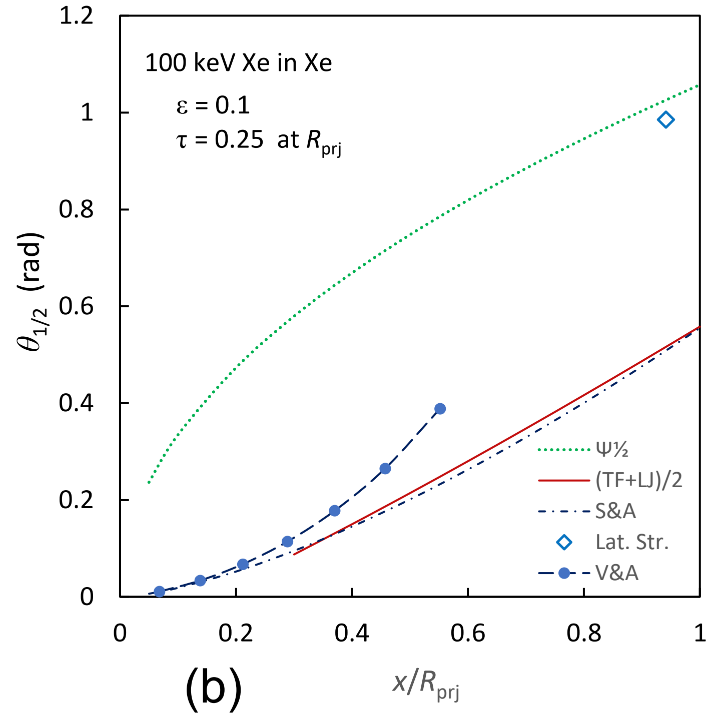

Fig. 3. Half width (HWHM) of the angular distribution $\theta_{1/2}$ for (a) 135 keV Ar recoil in Ar, and (b) 100 keV Xe recoils in Xe as a function of the thickness x in the unit of the projected range R_{prj}. The solid curve indicates the middle value of Thomas-Fermi and Lentz-Jensen, (TF+LJ)/2 potentials, dot-dash curve shows the empirical form [27], closed circles with dashed curve show the inclusion of the energy-loss effect [24]. The dotted curve is the Bohr-Williams approximation and the open diamond show the estimate using the range and the lateral straggling obtained from SRIM [16]. The results shown in Fig. (b) basically apply also for CsI crystal.

Scaling & References

$$\varepsilon = a_s / b = a_s \cdot \left(2a_0 \frac{R_\infty}{E} Z_1 Z_2 \frac{A_1 + A_2}{A_2} \right)^{-1}$$

$$\rho = RN \cdot 4\pi a_s^2 \frac{A_1 A_2}{(A_1 + A_2)^2}$$

$$\tau = \frac{a_s^2}{r_s^2} n_c = \pi a_s^2 N x$$

$$\vartheta = \theta \frac{\varepsilon}{2} \frac{A_1 + A_2}{A_2} \qquad u = \pi a_s^2 N \frac{E a_s}{2 Z_1 Z_2} \ell$$

a_s : screening radius
b : impact parameter
$a_0 = 0.529 \times 10^{-8}$ cm
$R_\infty = e^2/(2a_0) \approx 13.6$ eV

$r_0 \approx N^{-1/3}/2$
n_c : no. of collisions
$\ell = (y^2 + x^2)^{1/2}$

$$a_s = 0.8853 a_0 \cdot (Z_1^{2/3} + Z_2^{2/3})^{1/2}$$

References

1. Hitachi, Mozumder, Nakamura, *Energy deposition on nuclear emulsion by slow recoil ions for directional dark matter searches*. Phys. Rev. D 105, 063014 (2022).
2. L. Meyer, Phys. Stat. Sol. (b) 44, 253 (1971).
3. P. Sigmund and K.B. Winterbon, NIM 119, 541 (1974).
4. J. E. Valdés and N.R. Arista, Phys. Rev. A 49, 2690 (1994).
5. A.D. Marwick and P. Sigmund, NIM 126, 317-232 (1975).
6. G. Sidenius and N. Andersen, NIM 128, 271-276 (1975).
7. K.B. Winterbon et al. Mat. Fys. Medd. Dan. Vid. Selsk.37, no.14, 1-73 (1970).
8. H.E. Schiøtt, Mat. Fys. Medd. Dan. Vid. Selsk. 35, no.9, 1-20 (1966).

$Z_1 \neq Z_2$

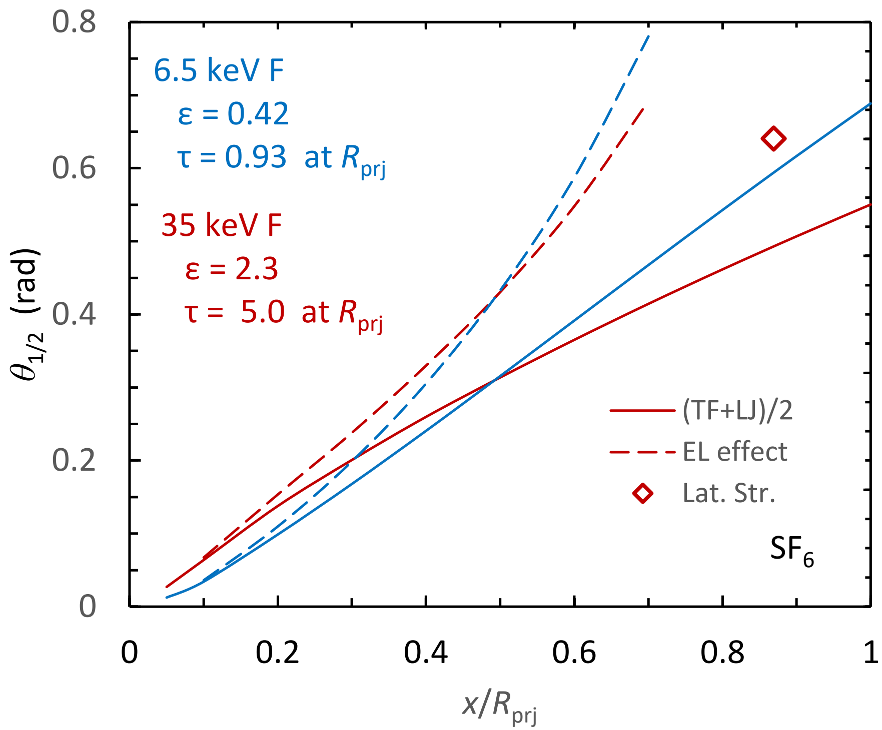

$\theta_{½}$ for 6.5 keV and 35 keV F recoils in SF_6 a function of the thickness x.

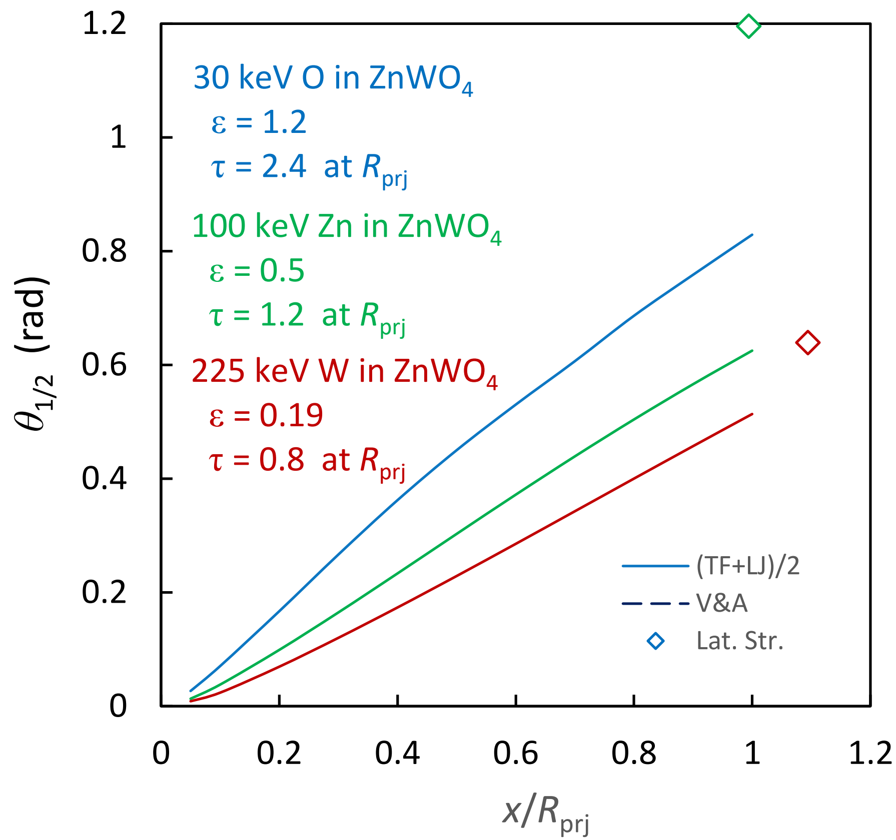

$\theta_{½}$ for 30 keV O, 100 keV Zn and 225 keV W recoils in $ZnWO_4$ crystal as a function of the thickness x.

q_{nc} の評価が難しい

Monte Carlo Simulations

Corturier et al. JCAP 2017
SRIM simulation

$1000\ \mathrm{GeV/c^2}\ \ \mathrm{WIMP}$

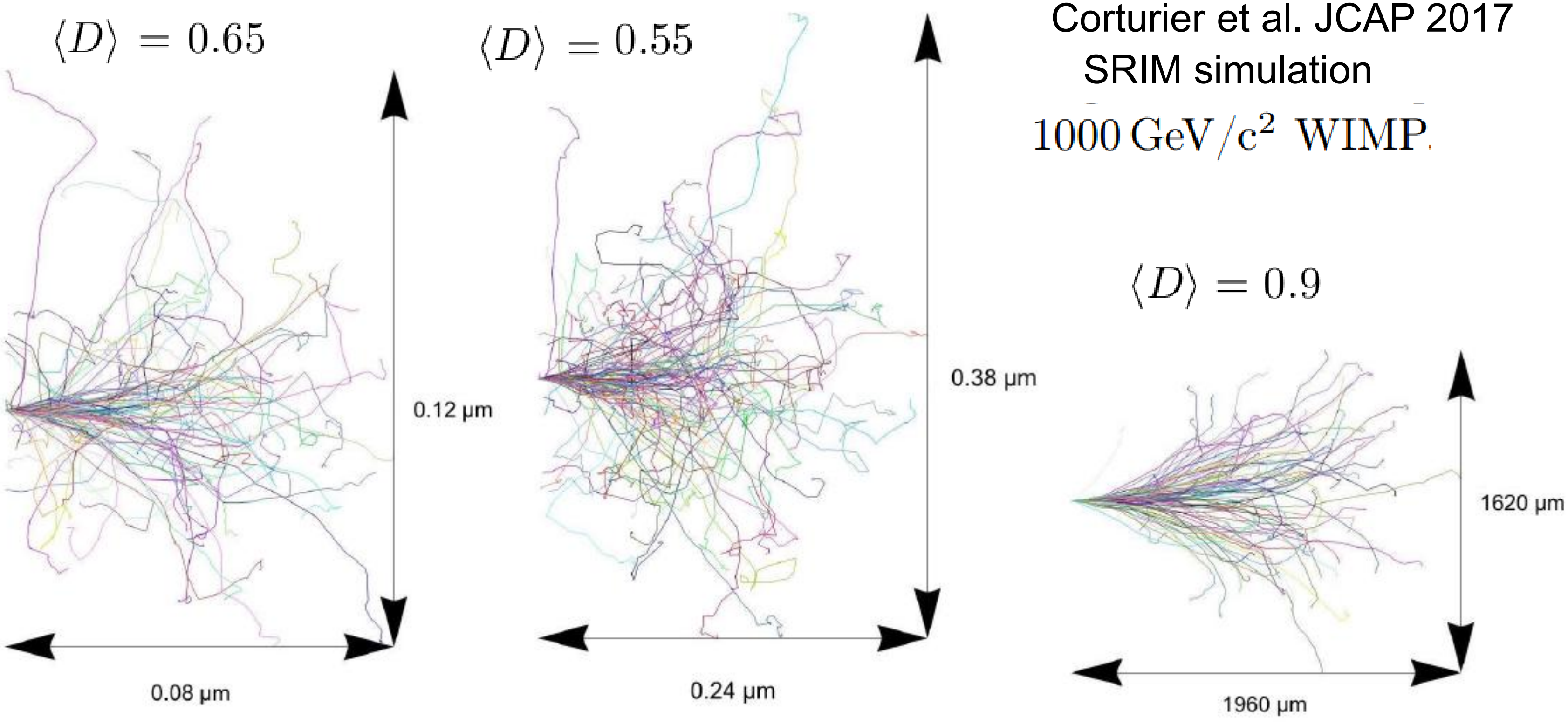

O in Crystal (29keV) | C in Emulsion (22keV) | F in TPC (34keV)

$$D = \frac{\langle \cos(\theta) \cdot \Delta E \rangle_{\mathrm{track}}}{\langle \Delta E \rangle_{\mathrm{track}}}$$

飛跡の3D分布。幹のみで枝は考慮されていない？
角度広がりを得るには一手間必要？

注) 平均した飛跡と個々の飛跡はかなり違う。

発光効率・電離収率

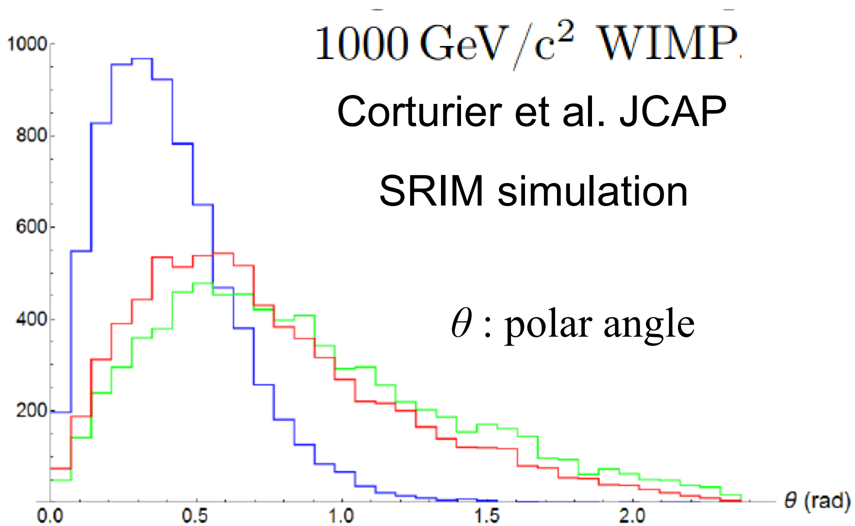
1000 GeV/c² WIMP
Corturier et al. JCAP
SRIM simulation
θ : polar angle
1000
800
600
400
200
0.0
0.5
1.0
1.5
2.0
θ (rad)

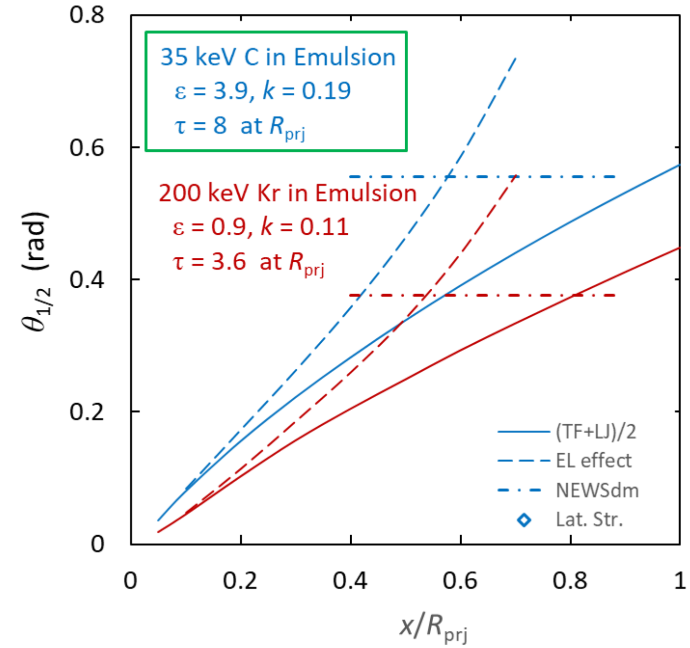
35 keV C in Emulsion
ε = 3.9, k = 0.19
τ = 8 at R_prj
200 keV Kr in Emulsion
ε = 0.9, k = 0.11
τ = 3.6 at R_prj
(TF+LJ)/2
EL effect
NEWSdm
Lat. Str.
θ_1/2 (rad)
x/R_prj

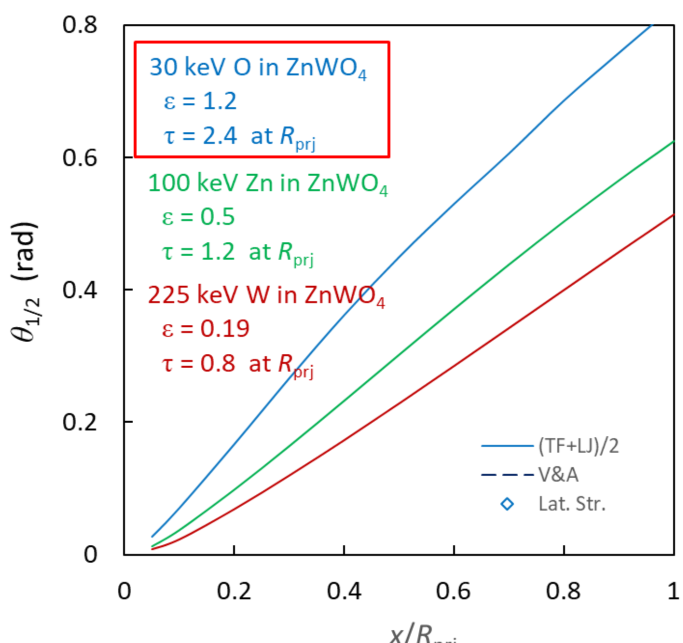
30 keV O in ZnWO4
ε = 1.2
τ = 2.4 at R_prj
100 keV Zn in ZnWO4
ε = 0.5
τ = 1.2 at R_prj
225 keV W in ZnWO4
ε = 0.19
τ = 0.8 at R_prj
(TF+LJ)/2
V&A
Lat. Str.
θ_1/2 (rad)
x/R_prj

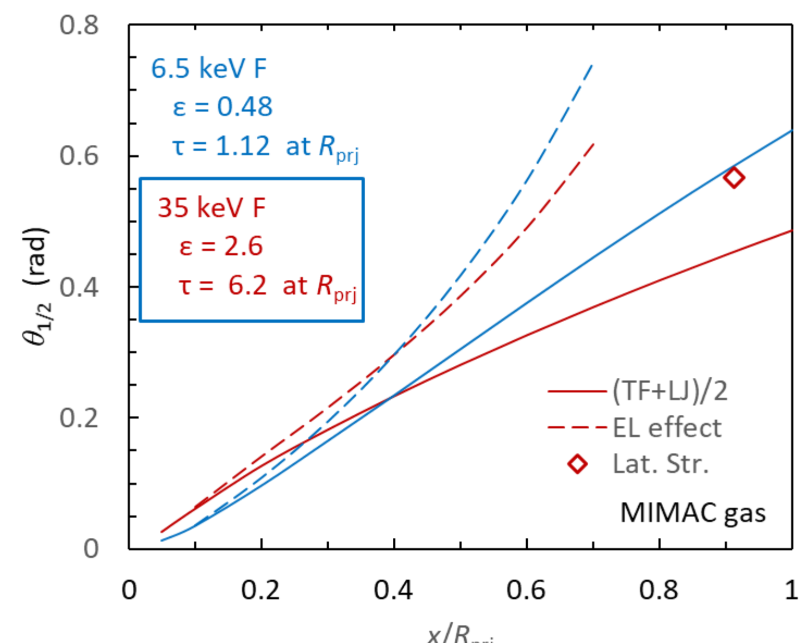
6.5 keV F
ε = 0.48
τ = 1.12 at R_prj
35 keV F
ε = 2.6
τ = 6.2 at R_prj
(TF+LJ)/2
EL effect
Lat. Str.
MIMAC gas
θ_1/2 (rad)
x/R_prj

Monte Carlo Simulations

MIMAC gas **Drift Direction**

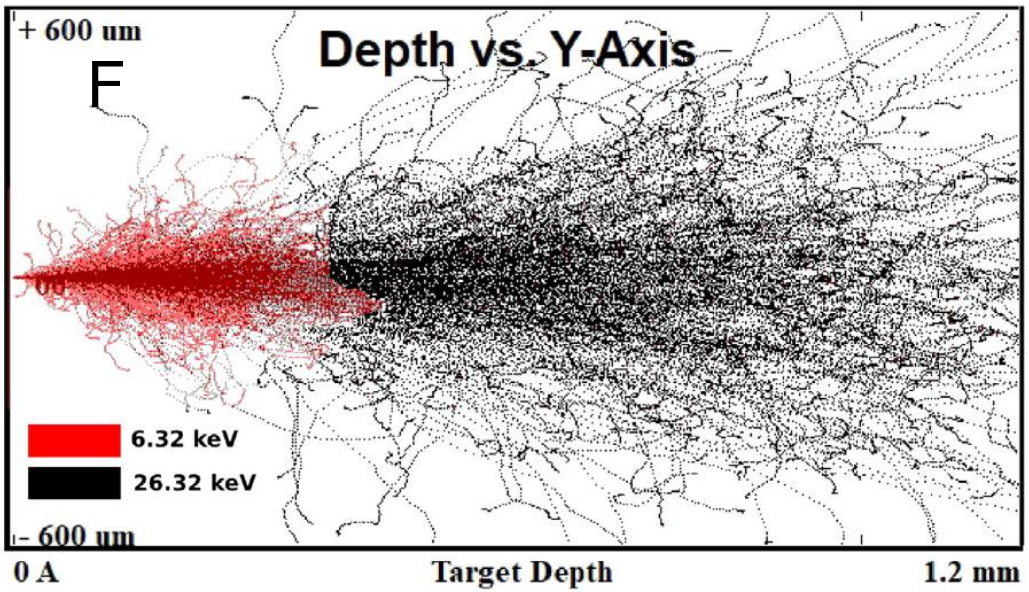

Tao, MIMAC, NIM A 985, 164569 (2021)

標準理論

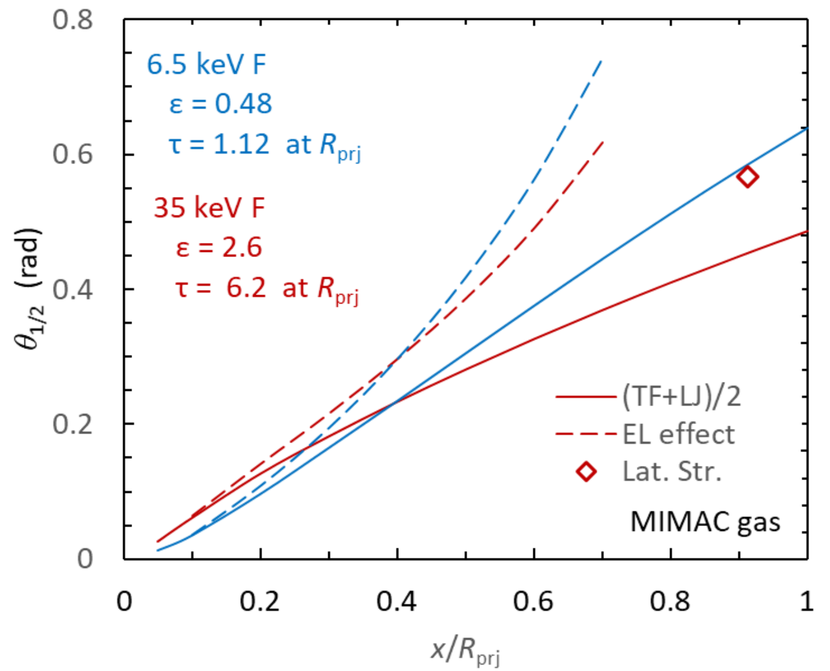

$\theta_{1/2}$ for 6.5 keV and 35 keV F recoils in MIMAC gas as a function of the thickness x.

MC Simulation

多くの event

$\theta_{1/2}$ は得られる　$E\eta$ 分布は難しい

測定されるのは event 毎

Nuclear Emulsion

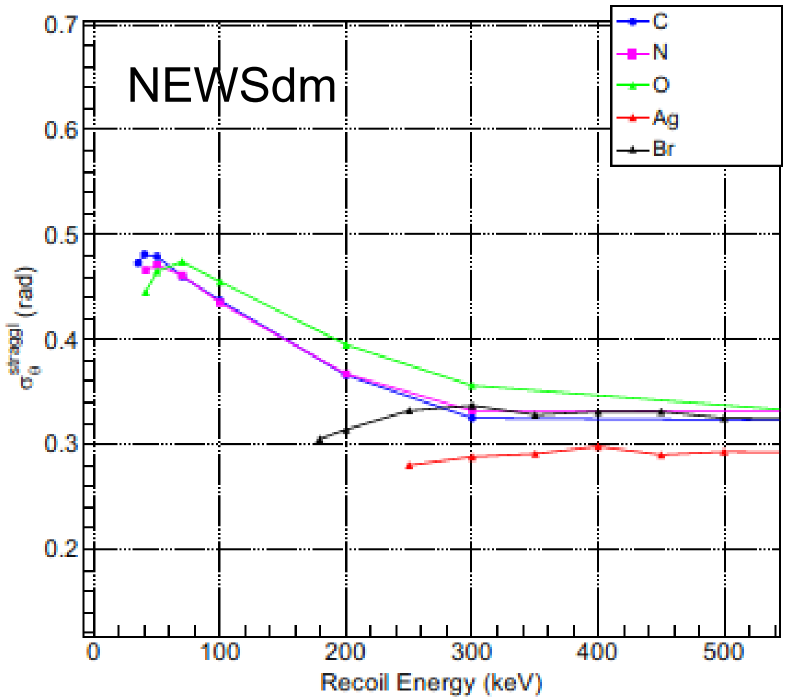

Fig. 2 Angular deviation due to the straggling of nuclei in a target. A 100 nm threshold on the range of the recoil track i

SRIM Command: "Ion Ranges (3D)"

TRIM track generator MC program

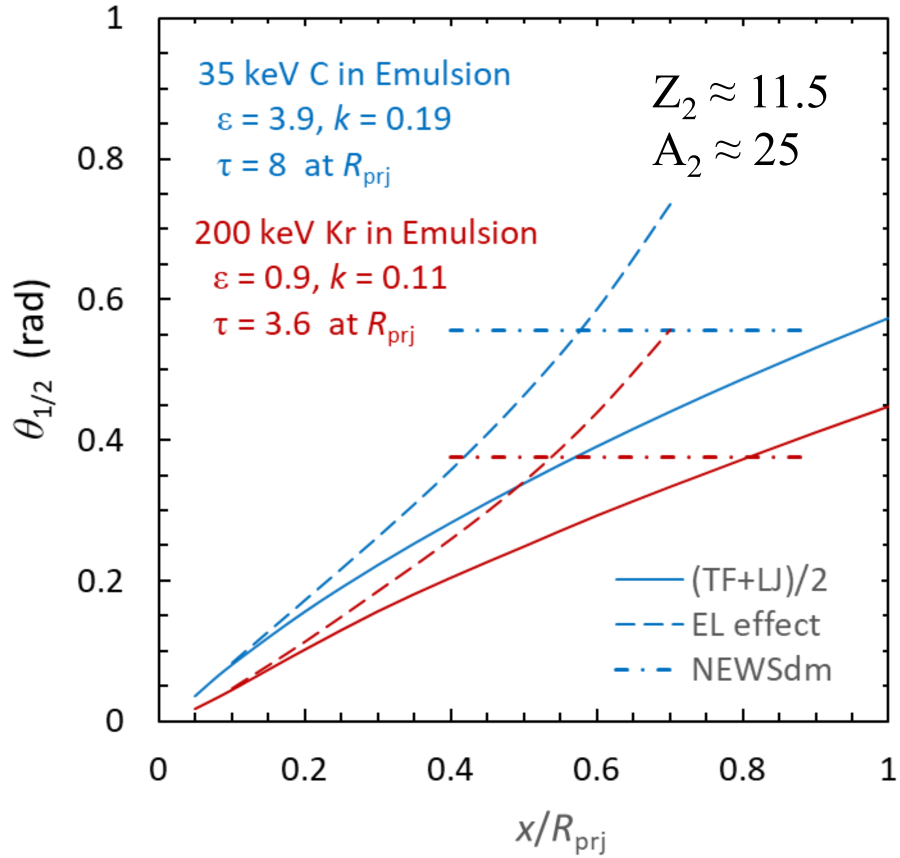

$\theta_{½}$ for 35 keV C recoils and 200 keV Kr recoils in nuclear emulsion as a function of the thickness x.